Physical Review & Research International
1(3): 74-105, 2011

SCIENCEDOMAIN *international*
www.sciencedomain.org

Phase and Ellipticity Dependence of the Photoelectron Angular Distribution in Non Resonant Three Photon Ionization of Atomic Hydrogen

Mamadou Faye[1]*

[1]Département de Physique, Faculté des Sciences et Techniques, Université Cheikh Anta Diop, Boulevard Martin Luther King (Corniche Ouest) BP. 5005 - Dakar - Fann - Sénégal.

Research Article

Received 20th May 2011
Accepted 20th June 2011
Online Ready 28th June 2011

ABSTRACT

We studied the ellipticity and the dependence on the phase lag (lead) (between the semi major and the semi minor axes of the field components) of the photoelectron angular distribution (PAD) in the non resonant three photon ionization of atomic hydrogen. The exact analytical expressions for azimuthal PAD for 1s, 2s, 3s, 2p, 3p and 3d, initial states, are given.

In comparison with dipole-dipole transitions, the number of quantum paths increases from: two to three for s-states; three to six for p-states; four to seven for d-states; while the number of angular coefficients goes from four to six, with two asymmetric terms. It is important that these asymmetric terms giving rise to the elliptic dichroism (ED), are only constituted with the imaginary part of the interference associated to the authorized channels leading to final states. Using the ED expression, we have established the phase shift isolation's equation for $l=0$ instead of $l=0,1$, initial states, previously. Similarly, it is notable that, the submagnetic levels, $m=0$ for $l=1$; $m=\pm1$, for $l=2$, initial states, do not contribute to the PAD.

Numerical evaluation of the angular coefficients is given for each state. The PAD shapes and the ED signals have been analyzed. It is found that, the maxima or the minima and the directions, of the PAD (1s, 2s, 3s, 3p), depend on the competing angular coefficients, which in return are affected by the interference terms. It is interesting to note that ,the asymmetric terms contribute only when the PAD maxima are shifted from the semi major or semi minor axes(2p,3d);and the isotropic shape(1s,2s,2p,3p,3d) is strongly dependent on the isotropic term. It is also observed that, when the photoelectron has a preference for the left handed or

**Corresponding author: Email: mamadou.faye@ucad.edu.sn;*

the right handed, the azimuthal detection difference between these two limit angles is reduced of one half than that obtained for dipole-dipole transitions. The highest ED signal (2p, 3p), occurs from the combination of the strong contributing asymmetric terms with the competing four first PAD terms. Besides, for 1s initial state, a nonzero ED signal is observed, at a particular value of the phase lag matching the phase shifts difference, for nearly circularly and nearly linearly polarized light.

Keywords: Phase lag; ellipticity; multiphoton; ionization; angular distribution; dichroism;

1. INTRODUCTION

Chirality, or handedness, refers to whether a system likes a left or a right handed screw. In quantum mechanics, the left or right handedness of a molecule or an atom can be identified by considering its interaction with a polarized light beam. The violation of the left - right symmetry leads to dichroism, and is usually observed for chiral molecules, (Huttunen, 2011; Persoons, 2011). Please modify the reference presentation in the text like this

For non chiral systems, since the surprising observation of the circular dichroism in the one photon double ionization of Helium (Viefhaus, 1996), researchers have paid much attention to dichroism in these systems (Andrei, 2004). Besides circular dichroism, the elliptic one seems to be much more fascinating. Thirty four years ago, Bouchiat and Bouchiat (1997) using an elliptically polarized photon to test parity violation in Cesium atoms, observed the existence of the Glashow, Weinberg and Salam's Z^0 vector boson.

Furthermore, Fifirig and Florescu (1998) and Fifirig (2002), in the case of two colour three photon ionization of Hydrogen atom; Dulieu et al. (1995) in the case of three and four photo-detachment of halogen negative ions, have studied the angular distributions by using elliptically polarized photons. These studies have not taken into account, in addition to the elliptic angle χ, the phase shift δ between the x-semimajor and the y-semiminor elliptic axes of the field components, i.e., when the y field component lags behind or leads the x component by δ degrees. The importance of this phase lies, by contrast to the usual harmonic phase control Fifirig (2002), in the possibility to observe a nonzero dichroism, if one considers e.g. the typical value of the ellipticity corresponding to circularly polarized light for which it vanishes, or one approaches linearly polarized light by doing $\delta \to 0$.

Recently, we studied the angular distributions in the cases of: three photons linearly and circularly polarized Faye et al. (2010) and two photon elliptically polarized Faye and Wane (2011a, 2011b).

In the present, we intend to extend these studies to the case of three photon elliptically polarized where some differences occur: firstly, as one can see below, for any state, the angular distribution of the emitted electron depends on the ϕ azimuthal angle; that is not case as described by Faye et al. (2010); secondly, it is notable, in addition to the presence of the quadratic and the real part of the interference, terms, associated to the quantum paths leading to the final states, that occurs at the same time, the imaginary part of the interference terms associated to these quantum paths. With respect to Faye and Wane (2011a) the number of opened channels increases from four to eight; while the contributing

angular coefficients enter two new terms with one asymmetric. As a consequence, these two asymmetric terms can strongly affect positively or negatively the dichroism. Besides, an important feature is, using the phase lag, the direct obtention of the phase shifts continua, independently of the radial transition matrix elements, from states of orbital quantum numbers *l=0* instead of *l=0,*1. These results of determining accurate continuum phase shifts would be of great interest for experimentalists (Gohedusen and Zimmermann, 1998; Nakajima, 2000).

How these angular coefficients are made from these various authorized channels? This question must not be avoided even if multiphoton angular distribution calculations always imply intricate calculations especially for initial states different of the most considered *l=0* ones.

Furthermore, to resolve the difficulty of the integration over the continuum for the evaluation of the radial transition matrix elements of the dipole operator between complete sets of atomic states (discrete as well continuum), we use here, the implicit summation technique as described by Faye et al. (2010) instead of the Integral representation of the Coulomb Green function used by Faye et al., (2003); Faye (2011).

In section 2, we establish the analytical expressions of the partial transition amplitudes appearing in the angular distribution for elliptically polarized light and we derive the corresponding azimuthal elliptically angular coefficients A_0, A_2, A_4, A_6, B_2 and B_4 for *l = 0* , *l*=1 and *l=2* quantum orbital numbers initial states ;in section 3,the analytical expressions for the asymmetric terms are established for the two parameters χ and δ; in section 4, we discuss our numerical results for 1s; 2s and 2p; 3s, 3p and 3d; initial states. We conclude in section 5. In the appendix we give the explicit expressions occurring in the development of the two asymmetric terms b_2 and b_4 for each state of orbital quantum number *l=0,*1,*2*.

2. ANGULAR DISTRIBUTION CALCULATIONS

Within the framework of the perturbation theory and of the dipole approximation, the differential cross section for non resonant three photon ionization (or detachment) has the general from Faye et al. (2010) in atomic units:

$$\frac{1}{I^2}\frac{d\sigma}{d\Omega}=\frac{\alpha}{4\pi I_0^2}\left|\sum_{s_1}\sum_{s_2}\frac{\langle f|\vec{\varepsilon}.\vec{r}|s_2\rangle\langle s_2|\vec{\varepsilon}.\vec{r}|s_1\rangle\langle s_1|\vec{\varepsilon}.\vec{r}|i\rangle}{(E_i-E_{s_2}+2E_p)(E_i-E_{s_1}+E_p)}\right|^2 E_p\,k_e a_0^2 \qquad (1)$$

where α is the fine structure constant, E_p and k_e are respectively the energy of the incident radiation and the momentum of the ejected electron, E_i , E_{s_1} ,and E_{s_2} are the energies of the initial and intermediate atomic states ; I is the radiation intensity in W/cm^2, I_0 = 7.019.10^{16} W/cm^2 ; I_0 is the unit of field strength and a_0 is the Bohr radius.

Writing the initial, intermediate and final states as described by Faye et al. (2010) and assuming the polarization $\vec{\varepsilon}$ to be (Faye and Wane, 2011):

$$\vec{\varepsilon} = \cos\zeta\,\vec{e}_x + i\sin\zeta\,\vec{e}_y \qquad (2)$$

with:

$$\cos\zeta = \frac{1}{\left(1+\tan^2\chi\sin^2\delta\right)^{1/2}}; \qquad \sin\zeta = \frac{\tan\chi\sin\delta}{\left(1+\tan^2\chi\sin^2\delta\right)^{1/2}}$$

where $\vec{e}_x$ and $\vec{e}_y$ are respectively the unit vectors of the semimajor and semiminor axes; χ is the elliptic angle ($-\pi/2 \le \chi \le \pi/2$), while δ is the phase lag (lead) between the semimajor and the semiminor field components ($-\pi \le \delta \le \pi$); Eq.(1) can be rewritten for any initial state characterized by its n-principal ; *l* - orbital and *m* - magnetic quantum numbers as :

$$\frac{1}{I^2}\frac{d\sigma_{nl}}{d\Omega} = \frac{\pi^2\alpha\,a_0^2E_p}{(2l+1)8I_0^2}\sum_{m=-l}^{+l}\left|M_{l+3}^{\zeta} + M_{l+1}^{\zeta} + M_{l-1}^{\zeta} + M_{l-3}^{\zeta}\right|^2 \qquad (3)$$

where the expressions of the partial transition amplitudes M_L read :

$$M_{l+3}^{\zeta} = (-i)^{l+3}e^{i\delta_{l+3}}T_{l+1,l+2,l+3}\Big\{(\cos\zeta+\sin\zeta)^3C_{l+3,m+3}^{l+1,l+2}Y_{l+3}^{m+3}(\hat{k}_e)$$
$$+3\cos2\zeta(\cos\zeta+\sin\zeta)C_{l+3,m+1}^{l+1,l+2}Y_{l+3}^{m+1}(\hat{k}_e)+3\cos2\zeta(\cos\zeta-\sin\zeta)C_{l+3,m-1}^{l+1,l+2}Y_{l+3}^{m-1}(\hat{k}_e)$$
$$+(\cos\zeta-\sin\zeta)^3C_{l+3,m-3}^{l+1,l+2}Y_{l+3}^{m-3}(\hat{k}_e)\Big\} \qquad (4)$$

$$M_{l+1}^{\zeta} = (-i)^{l+1}e^{i\delta_{l+1}}\Big\{(\cos\zeta+\sin\zeta)^3C_{l+1,m+3}Y_{l+1}^{m+3}(\hat{k}_e)\left[\frac{T_{l+1,l,l+1}}{(2l+1)(2l+3)}+\frac{T_{l+1,l+2,l+1}}{(2l+3)(2l+5)}\right.$$
$$\left.\frac{T_{l-1,l,l+1}}{(2l+1)(2l-1)}\right]+\cos2\zeta(\cos\zeta+\sin\zeta)Y_{l+1}^{m+1}(\hat{k}_e)\left[C_{l+1,m+1}^{l+1,l}\frac{T_{l+1,l,l+1}}{(2l+1)(2l+3)}\right.$$
$$\left.+C_{l+1,m+1}^{l+1,l+2}\frac{T_{l+1,l+2,l+1}}{(2l+3)(2l+5)}+C_{l+1,m+1}^{l-1,l}\frac{T_{l-1,l,l+1}}{(2l+1)(2l-1)}\right]$$
$$+\cos2\zeta(\cos\zeta-\sin\zeta)Y_{l+1}^{m-1}(\hat{k}_e)\left[C_{l+1,m-1}^{l+1,l}\frac{T_{l+1,l,l+1}}{(2l+1)(2l+3)}+C_{l+1,m-1}^{l+1,l+2}\frac{T_{l+1,l+2,l+1}}{(2l+3)(2l+5)}\right.$$
$$\left.+C_{l+1,m-1}^{l-1,l}\frac{T_{l-1,l,l+1}}{(2l+1)(2l-1)}\right]+(\cos\zeta-\sin\zeta)^3C_{l+1,m-3}Y_{l+1}^{m-3}(\hat{k}_e)\left[\frac{T_{l+1,l,l+1}}{(2l+1)(2l+3)}\right.$$
$$\left.+\frac{T_{l+1,l+2,l+1}}{(2l+3)(2l+5)}+\frac{T_{l-1,l,l+1}}{(2l+1)(2l-1)}\right]\Big\} \qquad (5)$$

$$M_{l-1}^{\zeta} = -(-i)^{l-1}e^{i\delta_{l-1}}\Big\{(\cos\zeta+\sin\zeta)^3C_{l-1,m+3}Y_{l-1}^{m+3}(\hat{k}_e)\left[\frac{T_{l+1,l,l-1}}{(2l+1)(2l+3)}+\frac{T_{l-1,l,l-1}}{(2l+1)(2l-1)}\right.$$

$$\frac{T_{l-1,l-2,l-1}}{(2l-1)(2l-3)}\Bigg]+\cos 2\zeta(\cos\zeta+\sin\zeta)Y_{l-1}^{m+1}(\hat{k}_e)\Bigg[C_{l-1,m+1}^{l+1,l}\frac{T_{l+1,l,l-1}}{(2l+1)(2l+3)}$$
$$+C_{l-1,m+1}^{l-1,l}\frac{T_{l-1,l,l-1}}{(2l+1)(2l-1)}+C_{l-1,m+1}^{l-1,l-2}\frac{T_{l-1,l-2,l-1}}{(2l-1)(2l-1)}\Bigg]+\cos 2\zeta(\cos\zeta-\sin\zeta)Y_{l-1}^{m-1}(\hat{k}_e)$$
$$\times\Bigg[C_{l-1,m-1}^{l+1,l}\frac{T_{l+1,l,l-1}}{(2l+1)(2l+3)}+C_{l-1,m-1}^{l-1,l}\frac{T_{l-1,l,l-1}}{(2l+1)(2l-1)}+C_{l-1,m-1}^{l-1,l-2}\frac{T_{l-1,l-2,l-1}}{(2l-1)(2l-3)}\Bigg]$$
$$+(\cos\zeta-\sin\zeta)^3C_{l-1,m-3}Y_{l-1}^{m-3}(\hat{k}_e)\Bigg[\frac{T_{l+1,l,l-1}}{(2l+1)(2l+3)}+\frac{T_{l-1,l,l-1}}{(2l-1)(2l+1)}+\frac{T_{l-1,l-2,l-1}}{(2l-1)(2l-3)}\Bigg]\Bigg\} \quad (6)$$

$$M_{l-3}^{\zeta}=(-i)^{l-3}e^{i\delta_{l-3}}T_{l-1,l-2,l-3}\Big\{(\cos\zeta+\sin\zeta)^3C_{l-3,m+3}^{l-1,l-2}Y_{l-3}^{m+3}(\hat{k}_e)$$
$$+3\cos 2\zeta(\cos\zeta+\sin\zeta)C_{l-3,m+1}^{l-1,l-2}Y_{l-3}^{m+1}(\hat{k}_e)+3\cos 2\zeta(\cos\zeta-\sin\zeta)C_{l-3,m-1}^{l-1,l-2}Y_{l-3}^{m-1}(\hat{k}_e)$$
$$+(\cos\zeta-\sin\zeta)^3C_{l-3,m-3}^{l-1,l-2}Y_{l-3}^{m-3}(\hat{k}_e)\Big\} \quad (7)$$

where the coefficients $C_{L,M}^{\lambda_1\lambda_2}$ depend on the quantum numbers *l* and *m*; (θ,ϕ) define the direction k_e of the ejected electron momentum; $\delta_L=\arg\Gamma(L+1-ik_e^{-1})$ is the Coulomb phase shift associated with the different opened channels of final orbital momentum L and,

$$T_{\lambda_1\lambda_2,L}=\sum_{\nu_1\nu_2}\frac{\langle R_{k_eL}|r|R_{\nu_2\lambda_2}\rangle\langle R_{\nu_2\lambda_2}|r|R_{\nu_1\lambda_1}\rangle\langle R_{\nu_1\lambda_1}|r|R_{nl}\rangle}{(E_{nl}-E_{\nu_2\lambda_2}+2E_p)(E_{nl}-E_{\nu_1\lambda_1}+E_p)}$$

is the radial transition matrix element, Y_L^M, is the usual spherical harmonic.

We can give now give, for the case of plane polarization in the x-y plane (i. e., when $\theta = \pi/2$) the explicit analytical expressions for the angular distribution for *l=0*, 1, 2 initial states.

2.1 *l=0*, Initial States

Three channels are authorized for the ejected photoelectron:

1. $s\to p\to d\to k_e f$; 2 $.s\to p\to d\to k_e p$; 3. $s\to p\to s\to k_e d$

By substituting *l=0*, *m = 0* in Eqs. (4) and (5), one easily obtains from Eq. (3),in the case where $\theta=\pi/2$ i.e. in the x y plane which is perpendicular to the direction of propagation of the light:

$$\frac{1}{I^2}\frac{d\sigma_{ns}^{\zeta}}{d\Omega} = C_{ns}\left(A_{0,ns} + A_{2,ns}\cos 2\phi + A_{4,ns}\cos 4\phi + A_{6,ns}\cos 6\phi + B_{2,ns}\sin 2\phi + B_{4,ns}\sin 4\phi\right) \tag{8}$$

Where in the $A_{2p,nl}$(p=0,1,2,3) and $B_{2p',nl}$(p'=1,2) coefficients the first subscript *and 2p'* refers to the coefficients of the azimuthal angle ϕ occurring in the cosine and the sine respectively, while the second one nl refers to the initial state with principal and orbital quantum numbers n and l respectively; with: $C_{ns} = \frac{\pi\alpha a_0^2 E_p}{I_0^2}$

and:

$$A_{0,ns} = \frac{1}{32}|T_{123}|^2 + \cos^2 2\zeta\left\{-\frac{33}{5^2 8^2}|T_{123}|^2 + \frac{1}{72}|T_{101}|^2 + \frac{2}{3^2 5^2}|T_{121}|^2 + \frac{1}{45}\Re(T_{101}T_{121}^*)\right.$$
$$\left. - \frac{1}{80}\Re(T_{123}T_{101}^* e^{i(\delta_3-\delta_1)}) - \frac{1}{100}\Re(T_{123}T_{121}^* e^{i(\delta_3-\delta_1)})\right\}$$

$$A_{2,ns} = \cos 2\zeta\left\{-\frac{3}{160}|T_{123}|^2 + \frac{1}{24}\Re(T_{123}T_{101}^* e^{i(\delta_3-\delta_1)}) + \frac{1}{30}\Re(T_{123}T_{121}^* e^{i(\delta_3-\delta_1)})\right\}$$
$$+ \cos^2 2\zeta\left\{-\frac{1}{48}\Re(T_{123}T_{101}^* e^{i(\delta_3-\delta_1)}) - \frac{1}{60}\Re(T_{123}T_{121}^* e^{i(\delta_3-\delta_1)})\right\}$$
$$+ \cos^3 2\zeta\left\{-\frac{39}{2.5^2 8^2}|T_{123}|^2 + \frac{1}{72}|T_{101}|^2 + \frac{2}{3^2 5^2}|T_{121}|^2 + \frac{1}{45}\Re(T_{101}T_{121}^*)\right.$$
$$\left. + \frac{1}{80}\Re(T_{123}T_{101}^* e^{i(\delta_3-\delta_1)}) + \frac{1}{100}\Re(T_{123}T_{121}^* e^{i(\delta_3-\delta_1)})\right\}$$

$$A_{4,ns} = \cos^2 2\zeta\left\{-\frac{3}{5.8^2}|T_{123}|^2 + \frac{1}{48}\Re(T_{123}T_{101}^* e^{i(\delta_3-\delta_1)}) + \frac{1}{60}\Re(T_{123}T_{121}^* e^{i(\delta_3-\delta_1)})\right\}$$

$$A_{6,ns} = \frac{1}{2.8^2}\cos^3 2\zeta|T_{123}|^2$$

$$B_{2,ns} = \cos 2\zeta \sin 2\zeta\left\{-\frac{1}{48}\Im(T_{123}T_{101}^* e^{i(\delta_3-\delta_1)}) - \frac{1}{60}\Im(T_{123}T_{121}^* e^{i(\delta_3-\delta_1)})\right\}$$

$$B_{4,ns} = \cos^2 2\zeta \sin 2\zeta\left\{-\frac{1}{48}\Im(T_{123}T_{101}^* e^{i(\delta_3-\delta_1)}) - \frac{1}{60}\Im(T_{123}T_{121}^* e^{i(\delta_3-\delta_1)})\right\} \tag{9}$$

Where $\Re(A.B^*)$ and $\Im(A.B^*)$ denote the real and the imaginary parts of the product of the variable A by the complex conjugated of the variable B.

2.2 *l*= 1, Initial States

The number of opened channels increases and reaches six:

1. $p \to d \to f \to k_e g$; 2. $p \to d \to f \to k_e d$; 3. $p \to d \to p \to k_e d$;

4. $p \to d \to p \to k_e s$; 5 $.p \to s \to p \to k_e d$; 6 $.p \to s \to p \to k_e s$

Putting *l=1* in Eqs. (4), (5) and (6) and successively *m = 1, -1* and *0*; we note that the magnetic sublevel *m=0*, does not contribute in Eq.(3). We obtain the same form as in Eq. (8), i.e.,

$$\frac{1}{I^2}\frac{d\sigma_{np}^{\zeta}}{d\Omega} = C_{np}\left(A_{0,np} + A_{2,np}\cos 2\phi + A_{4,np}\cos 4\phi + A_{6,np}\cos 6\phi + B_{2,np}\sin 2\phi + B_{4,np}\sin 4\phi\right) \tag{10}$$

where, $C_{np} = \dfrac{\pi\alpha a_0^2 E_p}{3I_0^2}$; and the angular coefficients $A_{0,np}$, $A_{2,np}$, $A_{4,np}$, $A_{6,np}$, $B_{2,np}$ and $B_{6,np}$ are given by:

$$A_{0,np} = \frac{75}{7^2 32}|T_{234}|^2 + \frac{3}{16}\left|\frac{T_{212}}{15} + \frac{T_{232}}{35} + \frac{T_{012}}{3}\right|^2 - \frac{1}{4^2 35}\Re(T_{234}T_{212}^* e^{i(\delta_4-\delta_2)})$$
$$-\frac{3}{4^2 7^2 5}\Re(T_{234}T_{232}^* e^{i(\delta_4-\delta_2)}) - \frac{1}{4^2 7}\Re(T_{234}T_{012}^* e^{i(\delta_4-\delta_2)}) + \cos^2 2\zeta\left\{-\frac{369}{5^2 8^2 7}|T_{234}|^2\right.$$
$$+\frac{239}{3^3 5^2 32}|T_{212}|^2 + \frac{207}{5^2 7.96}|T_{232}|^2 - \frac{7}{3^3 32}|T_{012}|^2 + \frac{33}{5^2 56}\Re(T_{212}T_{232}^*) + \frac{13}{3^3 5.24}\Re(T_{212}T_{012}^*)$$
$$+\frac{9}{35.16}\Re(T_{232}T_{012}^*) + \frac{1}{8^2 3}\left|\frac{16}{15}T_{210} + \frac{4}{3}T_{010}\right|^2 - \frac{57}{32.5^2 7}\Re(T_{234}T_{212}^* e^{i(\delta_4-\delta_2)})$$
$$-\frac{9}{160}\Re(T_{234}T_{232}^* e^{i(\delta_4-\delta_2)}) - \frac{3}{1120}\Re(T_{234}T_{012}^* e^{i(\delta_4-\delta_2)}) + \frac{3}{5^2 28}\Re(T_{234}T_{210}^* e^{i(\delta_4-\delta_0)})$$
$$+\frac{3}{4^2 35}\Re(T_{234}T_{010}^* e^{i(\delta_4-\delta_0)}) - \frac{4}{3^3 54}\Re(T_{212}T_{210}^* e^{i(\delta_2-\delta_0)}) - \frac{1}{3^2 5^2 28}\Re(T_{232}T_{210}^* e^{i(\delta_2-\delta_0)})$$
$$\left.-\frac{1}{16.3^2 35}\Re(T_{232}T_{010}^* e^{i(\delta_2-\delta_0)}) - \frac{1}{180}\Re(T_{012}T_{210}^* e^{i(\delta_2-\delta_0)}) - \frac{1}{3^3 16}\Re(T_{012}T_{010}^* e^{i(\delta_2-\delta_0)})\right\}$$

$$A_{2,np} = \cos 2\zeta\left\{-\frac{171}{5.7^2 32}|T_{234}|^2 + \frac{1}{150}|T_{212}|^2 + \frac{27}{5^2 7^2.8}|T_{232}|^2\right.$$
$$+\frac{1}{24}|T_{012}|^2 + \frac{13}{5^2 56}\Re(T_{212}.T_{232}^*) + \frac{1}{24}\Re(T_{212}T_{012}^*) + \frac{1}{28}\Re(T_{232}T_{012}^*)$$
$$+\frac{401}{48.5^2 7}\Re(T_{234}T_{212}^* e^{i(\delta_4-\delta_2)}) + \frac{951}{16.5^2 7^2}\Re(T_{234}T_{232}^* e^{i(\delta_4-\delta_2)}) + \frac{71}{1680}\Re(T_{234}T_{012}^* e^{i(\delta_4-\delta_2)})$$
$$-\frac{1}{210}\Re(T_{234}T_{210}^* e^{i(\delta_4-\delta_0)}) - \frac{1}{168}\Re(T_{234}T_{010}^* e^{i(\delta_4-\delta_0)}) + \frac{2}{225}\Re(T_{212}T_{210}^* e^{i(\delta_2-\delta_0)})$$
$$+\frac{1}{90}\Re(T_{212}T_{010}^* e^{i(\delta_2-\delta_0)}) + \frac{2}{525}\Re(T_{232}T_{210}^* e^{i(\delta_2-\delta_0)}) + \frac{1}{210}\Re(T_{232}T_{010}^* e^{i(\delta_2-\delta_0)})$$
$$\left.+\frac{2}{45}\Re(T_{012}T_{210}^* e^{i(\delta_2-\delta_0)}) + \frac{1}{18}\Re(T_{012}T_{010}^* e^{i(\delta_2-\delta_0)})\right\} + \cos^3 2\zeta\left\{\frac{261}{10.7^2 8^2}|T_{234}|^2 + \frac{1}{36}|T_{212}|^2\right.$$
$$+\frac{117}{5.7^2.4^2}|T_{232}|^2 + \frac{1}{3^2 4^2}|T_{012}|^2 + \frac{97}{1680}\Re(T_{212}.T_{232}^*) + \frac{19}{720}\Re(T_{212}T_{012}^*) + \frac{37}{840}\Re(T_{232}T_{012}^*)$$
$$-\frac{619}{8^2.5^2 21}\Re(T_{234}T_{212}^* e^{i(\delta_4-\delta_2)}) - \frac{1479}{8^2.5^2 7^2}\Re(T_{234}T_{232}^* e^{i(\delta_4-\delta_2)}) - \frac{103}{8^2 105}\Re(T_{234}T_{012}^* e^{i(\delta_4-\delta_2)})$$
$$-\frac{1}{70}\Re(T_{234}T_{210}^* e^{i(\delta_4-\delta_0)}) - \frac{1}{56}\Re(T_{234}T_{010}^* e^{i(\delta_4-\delta_0)}) + \frac{1}{90}\Re(T_{212}T_{210}^* e^{i(\delta_2-\delta_0)})$$
$$\left.+\frac{1}{72}\Re(T_{212}T_{010}^* e^{i(\delta_2-\delta_0)}) + \frac{1}{70}\Re(T_{232}T_{210}^* e^{i(\delta_2-\delta_0)})\right.$$

$$A_{4,np} = \cos^2 2\zeta\left\{-\frac{27}{7^2 160}|T_{234}|^2 + \frac{1}{2400}|T_{212}|^2 + \frac{27}{5^2 7^2.32}|T_{232}|^2 + \frac{1}{96}|T_{012}|^2\right.$$
$$+\frac{3}{700}\Re(T_{212}.T_{232}^*) + \frac{1}{60}\Re(T_{212}T_{012}^*) + \frac{9}{560}\Re(T_{232}T_{012}^*) - \frac{43}{3360}\Re(T_{234}T_{212}^* e^{i(\delta_4-\delta_2)})$$
$$-\frac{93}{160.7^2}\Re(T_{234}T_{232}^* e^{i(\delta_4-\delta_2)}) - \frac{13}{672}\Re(T_{234}T_{012}^* e^{i(\delta_4-\delta_2)}) + \frac{1}{60}\Re(T_{234}T_{210}^* e^{i(\delta_4-\delta_0)})$$
$$\left.+\frac{1}{48}\Re(T_{234}T_{010}^* e^{i(\delta_4-\delta_0)})\right\}$$

$$A_{6,np} = \cos^3 2\zeta\left\{-\frac{3}{8^2 14}|T_{234}|^2 + \frac{1}{8^2 5}\Re(T_{234}T_{212}^* e^{i(\delta_4-\delta_2)})\right.$$
$$\left.+\frac{3}{8^2 35}\Re(T_{234}T_{232}^* e^{i(\delta_4-\delta_2)}) + \frac{1}{8^2}\Re(T_{234}T_{012}^* e^{i(\delta_4-\delta_2)})\right\}$$

$$B_{2,np} = \cos 2\zeta \sin 2\zeta \Big\{ -\frac{13}{5^2 56}\Im(T_{212}T^*_{232}) - \frac{1}{24}\Im(T_{212}T^*_{012}) - \frac{1}{28}\Im(T_{232}T^*_{012})$$
$$-\frac{187}{4200}\Im(T_{234}T^*_{212}e^{i(\delta_4-\delta_2} - \frac{33}{700}\Im(T_{234}T^*_{232}e^{i(\delta_4-\delta_2)}) - \frac{11}{420}\Im(T_{234}T^*_{012}e^{i(\delta_4-\delta_2)})$$
$$+\frac{1}{420}\Im(T_{234}T^*_{210}e^{i(\delta_4-\delta_0)}) + \frac{1}{336}\Im(T_{234}T^*_{010}e^{i(\delta_4-\delta_0)}) - \frac{1}{225}\Im(T_{212}T^*_{210}e^{i(\delta_2-\delta_0)})$$
$$-\frac{1}{180}\Im(T_{212}T^*_{010}e^{i(\delta_2-\delta_0)}) - \frac{1}{525}\Im(T_{232}T^*_{210}e^{i(\delta_2-\delta_0)}) - \frac{1}{420}\Im(T_{232}T^*_{010}e^{i(\delta_4-\delta_2)})$$
$$-\frac{1}{36}\Im(T_{012}T^*_{010}e^{i(\delta_2-\delta_0)}) - \frac{1}{45}\Im(T_{012}T^*_{210}e^{i(\delta_2-\delta_0)}) \Big\}$$
$$B_{4,np} = \cos^2 2\zeta \sin 2\zeta \Big\{ -\frac{3}{700}\Im(T_{212}T^*_{232}) - \frac{1}{60}\Im(T_{212}T^*_{012}) - \frac{9}{560}\Im(T_{232}T^*_{012})$$
$$+\frac{47}{1680}\Im(T_{234}T^*_{212}e^{i(\delta_4-\delta_2} + \frac{3}{280}\Im(T_{234}T^*_{232}e^{i(\delta_4-\delta_2)}) + \frac{1}{168}\Im(T_{234}T^*_{012}e^{i(\delta_4-\delta_2)})$$
$$-\frac{1}{60}\Im(T_{234}T^*_{210}e^{i(\delta_4-\delta_0)}) - \frac{1}{48}\Im(T_{234}T^*_{010}e^{i(\delta_4-\delta_0)}) \Big\} \qquad (11)$$

which have the same form than Equation (9) except for $A_{2,np}$ where the second term related to $\cos^2 2\zeta$ disappears. We note in $B_{4,np}$ the lack of the contributing interference terms associated to quantum paths of final orbital momenta 2 and 0. We turn now to *l=2* initial state.

2.3 *l=2*, Initial States

Here the photoelectron can take seven opened channels:

1. $d \to f \to g \to k_e e$; 2. $d \to f \to g \to k_e f$; 3 $.d \to f \to d \to k_e f$;

4. $d \to f \to d \to k_e p$; 5 $.d \to p \to d \to k_e f$; 6 $.d \to p \to d \to k_e p$;

7. $d \to p \to s \to k_e p$

As a consequence the number of terms drastically increases.

By substituting *l=2*, in Eqs. (4) (5) and (6) and successively *m* = +*2* , *-2,* +1, -1 and *0* , and using the same process as for *l=0*, 1, we note that the magnetic sublevels *m=±*1 do not contribute to the PAD; after some tedious calculations Eq.(3) adopts the same form as Eq. (11), where:

the coefficient,

$$C_{3d} = \frac{\pi\alpha a_0^2 E_p}{5I_0^2}$$

and the angular coefficients $A_{0,3d}$, $A_{2,3d}$, $A_{4,3d}$, $A_{6,3d}$, $B_{2,3d}$ and $B_{4,3d}$ are given by:

$$A_{0,3d} = \frac{445}{7056}\left|T_{345}\right|^2 + \frac{279}{160}\left|\frac{T_{323}}{35} + \frac{T_{343}}{63} + \frac{T_{123}}{15}\right|^2 + \frac{1}{3920}\Re(T_{345}T_{321}^* e^{i(\delta_5-\delta_1)})$$
$$+ \frac{3}{20}\left|\frac{T_{321}}{35} + \frac{T_{121}}{15} + \frac{T_{101}}{3}\right|^2 - \frac{19}{3920}\Re(T_{345}T_{323}^* e^{i(\delta_5-\delta_3)}) - \frac{19}{1680}\Re(T_{345}T_{123}^* e^{i(\delta_5-\delta_3)})$$
$$- \frac{19}{7056}\Re(T_{345}T_{343}^* e^{i(\delta_5-\delta_3)}) + \frac{1}{1680}\Re(T_{345}T_{121}^* e^{i(\delta_5-\delta_1)}) + \frac{1}{336}\Re(T_{345}T_{101}^* e^{i(\delta_5-\delta_1)})$$
$$- \frac{9}{5^3 7^2}\Re(T_{323}T_{321}^* e^{i(\delta_3-\delta_1)}) - \frac{3}{5^3 7}\Re(T_{323}T_{121}^* e^{i(\delta_3-\delta_1)}) - \frac{3}{175}\Re(T_{323}T_{101}^* e^{i(\delta_3-\delta_1)})$$
$$- \frac{3}{525}\Re(T_{123}T_{321}^* e^{i(\delta_3-\delta_1)}) - \frac{1}{75}\Re(T_{123}T_{121}^* e^{i(\delta_3-\delta_1)}) - \frac{1}{25}\Re(T_{123}T_{101}^* e^{i(\delta_5-\delta_1)})$$
$$- \frac{1}{1225}\Re(T_{343}T_{321}^* e^{i(\delta_3-\delta_1)}) - \frac{1}{525}\Re(T_{343}T_{121}^* e^{i(\delta_3-\delta_1)}) - \frac{1}{105}\Re(T_{343}T_{101}^* e^{i(\delta_3-\delta_1)})$$
$$+ \cos^2 2\zeta\left\{-\frac{205}{4704}\left|T_{345}\right|^2 + \frac{1101}{5^2 7^2 8^2}\left|T_{323}\right|^2 + \frac{767}{5880}\left|T_{343}\right|^2 + \frac{9}{1600}\left|T_{123}\right|^2 + \frac{139}{7840}\Re(T_{323}T_{343}^*)\right.$$
$$+ \frac{117}{5600}\Re(T_{323}T_{123}^*) + \frac{27}{1120}\Re(T_{343}T_{123}^*) + \frac{51}{4900}\left|T_{321}\right|^2 + \frac{17}{1800}\left|T_{121}\right|^2 - \frac{1}{180}\left|T_{101}\right|^2$$
$$+ \frac{1}{50}\Re(T_{321}T_{121}^*) + \frac{1}{70}\Re(T_{321}T_{101}^*) + \frac{1}{90}\Re(T_{121}T_{101}^*) - \frac{41}{5.8^2 7^2}\Re(T_{345}T_{323}^* e^{i(\delta_5-\delta_3)})$$
$$- \frac{59}{4704}\Re(T_{345}T_{343}^* e^{i(\delta_5-\delta_3)}) - \frac{107}{8^2 420}\Re(T_{345}T_{123}^* e^{i(\delta_5-\delta_3)}) + \frac{3}{980}\Re(T_{345}T_{321}^* e^{i(\delta_5-\delta_1)})$$
$$+ \frac{3}{1120}\Re(T_{345}T_{121}^* e^{i(\delta_5-\delta_1)}) - \frac{177}{5^2 7^2 16}\Re(T_{323}T_{321}^* e^{i(\delta_3-\delta_1)}) - \frac{3}{350}\Re(T_{323}T_{121}^* e^{i(\delta_3-\delta_1)})$$
$$- \frac{3}{560}\Re(T_{323}T_{101}^* e^{i(\delta_3-\delta_1)}) - \frac{9}{980}\Re(T_{343}T_{321}^* e^{i(\delta_3-\delta_1)}) - \frac{3}{560}\Re(T_{343}T_{121}^* e^{i(\delta_3-\delta_1)})$$
$$\left. - \frac{3}{140}\Re(T_{343}T_{101}^* e^{i(\delta_3-\delta_1)}) - \frac{3}{350}\Re(T_{123}T_{321}^* e^{i(\delta_3-\delta_1)}) - \frac{3}{400}\Re(T_{123}T_{121}^* e^{i(\delta_3-\delta_1)})\right\}$$

$$A_{2,3d} = \cos 2\zeta\left\{-\frac{155}{8^2 7^2 2}|T_{345}|^2 - \frac{387}{5^3 7^2 32}|T_{323}|^2 - \frac{11}{7840}|T_{343}|^2 - \frac{3}{4000}|T_{123}|^2\right.$$
$$- \frac{71}{5^2 7^2 16}\Re(T_{323}T_{343}^*) - \frac{69}{5^2 112}\Re(T_{323}T_{123}^*) - \frac{51}{8400}\Re(T_{343}T_{123}^*) + \frac{51}{5^3 7^2 4}|T_{321}|^2$$
$$+ \frac{7}{1500}|T_{121}|^2 + \frac{1}{60}|T_{101}|^2 + \frac{6}{875}\Re(T_{321}T_{121}^*) + \frac{9}{350}\Re(T_{321}T_{101}^*) + \frac{2}{50}\Re(T_{121}T_{101}^*)$$
$$+ \frac{239}{7840}\Re(T_{345}T_{323}^* e^{i(\delta_5-\delta_3)}) + \frac{99}{1568}\Re(T_{345}T_{343}^* e^{i(\delta_5-\delta_3)}) + \frac{279}{4480}\Re(T_{345}T_{123}^* e^{i(\delta_5-\delta_3)})$$
$$- \frac{11}{3920}\Re(T_{345}T_{321}^* e^{i(\delta_5-\delta_1)}) - \frac{13}{5040}\Re(T_{345}T_{121}^* e^{i(\delta_5-\delta_1)}) - \frac{1}{1008}\Re(T_{345}T_{101}^* e^{i(\delta_5-\delta_1)})$$
$$- \frac{51}{5^3 7^2 8}\Re(T_{323}T_{321}^* e^{i(\delta_3-\delta_1)}) - \frac{3}{1750}\Re(T_{323}T_{121}^* e^{i(\delta_3-\delta_1)}) - \frac{9}{1400}\Re(T_{323}T_{101}^* e^{i(\delta_3-\delta_1)})$$
$$- \frac{1}{5^2 7^2}\Re(T_{343}T_{321}^* e^{i(\delta_3-\delta_1)}) - \frac{19}{5^2 3^2 56}\Re(T_{343}T_{121}^* e^{i(\delta_3-\delta_1)}) - \frac{2}{360}\Re(T_{343}T_{101}^* e^{i(\delta_3-\delta_1)})$$
$$\left.- \frac{3}{1750}\Re(T_{123}T_{321}^* e^{i(\delta_3-\delta_1)}) - \frac{7}{3000}\Re(T_{123}T_{121}^* e^{i(\delta_3-\delta_1)}) - \frac{1}{150}\Re(T_{123}T_{101}^* e^{i(\delta_3-\delta_1}\right)\Big\}$$
$$+ \cos^3 2\zeta\left\{\frac{195}{8^2 7^2 4}|T_{345}|^2 - \frac{597}{7^2 8^2 5^2 2}|T_{323}|^2 - \frac{97}{8^2 5^2 10}|T_{343}|^2 - \frac{21}{8^2 5^2 2}|T_{123}|^2\right.$$
$$+ \frac{449}{8^2 5^2 7^2 3}\Re(T_{323}T_{343}^*) - \frac{111}{8^2 5^2 7}\Re(T_{323}T_{123}^*) - \frac{99}{8^2 5^2 7}\Re(T_{343}T_{123}^*) - \frac{3}{5^3 56}|T_{321}|^2$$
$$- \frac{13}{4500}|T_{121}|^2 - \frac{1}{72}|T_{101}|^2 - \frac{3}{875}\Re(T_{321}T_{121}^*) - \frac{3}{140}\Re(T_{321}T_{101}^*) - \frac{1}{45}\Re(T_{121}T_{101}^*)$$
$$- \frac{29}{7^2 8^2 10}\Re(T_{345}T_{323}^* e^{i(\delta_5-\delta_3)}) - \frac{1}{196}\Re(T_{345}T_{343}^* e^{i(\delta_5-\delta_3)}) + \frac{37}{4480}\Re(T_{345}T_{123}^* e^{i(\delta_5-\delta_3)})$$
$$- \frac{97}{8^2 7^2 5}\Re(T_{345}T_{321}^* e^{i(\delta_5-\delta_1)}) - \frac{121}{8^2 3^2 35}\Re(T_{345}T_{121}^* e^{i(\delta_5-\delta_1)}) - \frac{19}{8^2 3^2 7}\Re(T_{345}T_{101}^* e^{i(\delta_5-\delta_1)})$$
$$+ \frac{33}{1960}\Re(T_{323}T_{321}^* e^{i(\delta_5-\delta_1)}) + \frac{3}{175}\Re(T_{323}T_{121}^* e^{i(\delta_3-\delta_1)}) + \frac{9}{700}\Re(T_{323}T_{101}^* e^{i(\delta_3-\delta_1)})$$
$$+ \frac{22}{5^2 7^2}\Re(T_{343}T_{321}^* e^{i(\delta_3-\delta_1)}) + \frac{109}{6300}\Re(T_{343}T_{121}^* e^{i(\delta_3-\delta_1)}) + \frac{4}{1750}\Re(T_{343}T_{101}^* e^{i(\delta_3-\delta_1)})$$
$$\left.+ \frac{113}{5600}\Re(T_{123}T_{121}^* e^{i(\delta_3-\delta_1)}) + \frac{47}{2400}\Re(T_{123}T_{121}^* e^{i(\delta_3-\delta_1)}) + \frac{37}{2400}\Re(T_{123}T_{101}^* e^{i(\delta_3-\delta_1)})\right\}$$

$$A_{4,3d} = \cos^2 2\zeta\left\{\frac{5}{5376}|T_{345}|^2 - \frac{261}{8^2 7^2 5^2}|T_{323}|^2 - \frac{57}{7^2 8^2 9}|T_{343}|^2 - \frac{9}{8^2 5^2}|T_{123}|^2\right.$$
$$- \frac{43}{7840}\Re(T_{323}T_{343}^*) - \frac{57}{5600}\Re(T_{323}T_{123}^*) - \frac{11}{1200}\Re(T_{343}T_{123}^*) + \frac{239}{8^2 7^2 10}\Re(T_{345}T_{323}^* e^{i(\delta_5-\delta_3)})$$
$$+ \frac{173}{8^2 7^2 3^2}\Re(e^{i(\delta_5-\delta_3)}T_{345}T_{343}^*) + \frac{83}{8^2 210}\Re(T_{345}T_{123}^* e^{i(\delta_5-\delta_3)}) + \frac{11}{560}\Re(T_{345}T_{321}^* e^{i(\delta_5-\delta_1)})$$
$$+ \frac{13}{720}\Re(T_{345}T_{121}^* e^{i(\delta_5-\delta_1)}) + \frac{1}{144}\Re(T_{345}T_{101}^* e^{i(\delta_5-\delta_1)}) + \frac{51}{7^2 5^2 16}\Re(T_{323}T_{321}^* e^{i(\delta_3-\delta_1)})$$
$$+ \frac{3}{700}\Re(T_{323}T_{121}^* e^{i(\delta_3-\delta_1)}) + \frac{9}{560}\Re(T_{323}T_{101}^* e^{i(\delta_3-\delta_1)}) + \frac{1}{490}\Re(T_{343}T_{321}^* e^{i(\delta_3-\delta_1)})$$
$$+ \frac{19}{5040}\Re(T_{343}T_{121}^* e^{i(\delta_3-\delta_1)}) + \frac{1}{63}\Re(T_{343}T_{101}^* e^{i(\delta_3-\delta_1)}) + \frac{1}{224}\Re(T_{123}T_{321}^* e^{i(\delta_3-\delta_1)})$$
$$\left. + \frac{1}{160}\Re(T_{123}T_{121}^* e^{i(\delta_3-\delta_1)}) + \frac{3}{160}\Re(T_{123}T_{101}^* e^{i(\delta_3-\delta_1)})\right\}$$

$$A_{6,3d} = \cos^3 2\zeta\left\{\frac{5}{2016}|T_{345}|^2 + \frac{45}{128}\left|\frac{T_{323}}{35} + \frac{T_{343}}{63} + \frac{T_{123}}{15}\right|^2 + \frac{37}{2240}\Re(T_{345}T_{321}^* e^{i(\delta_5-\delta_1)})\right.$$
$$\left. + \frac{37}{320}\Re(T_{345}T_{121}^* e^{i(\delta_5-\delta_1)}) + \frac{1}{8^2}\Re(T_{345}T_{101}^* e^{i(\delta_5-\delta_1)})\right\}$$

$$B_{2,3d} = \cos 2\zeta \sin 2\zeta\left\{-\frac{29}{5^2 7^2 16}\Im(T_{323}T_{343}^*) - \frac{51}{5^3 112}\Im(T_{323}T_{123}^*) - \frac{1}{350}\Im(T_{343}T_{123}^*)\right.$$
$$- \frac{6}{875}\Im(T_{321}T_{121}^*) - \frac{9}{350}\Im(T_{321}T_{101}^*) - \frac{2}{75}\Im(T_{121}T_{101}^*) - \frac{1831}{7^2 8^2 10}\Im(T_{345}T_{323}^* e^{i(\delta_5-\delta_3)})$$
$$- \frac{197}{8^2 7^2}\Im(e^{i(\delta_5-\delta_3)}T_{345}T_{343}^*) + \frac{701}{8^2 210}\Im(T_{345}T_{123}^* e^{i(\delta_5-\delta_3)}) + \frac{1}{280}\Im(T_{345}T_{321}^* e^{i(\delta_5-\delta_1)})$$
$$+ \frac{37}{3^2 1120}\Im(T_{345}T_{121}^* e^{i(\delta_5-\delta_1)}) + \frac{5}{504}\Im(T_{345}T_{101}^* e^{i(\delta_5-\delta_1)}) - \frac{3}{7^2 5^2 8}\Im(T_{323}T_{321}^* e^{i(\delta_3-\delta_1)})$$
$$- \frac{1}{700}\Im(T_{323}T_{121}^* e^{i(\delta_3-\delta_1)}) - \frac{13}{1400}\Im(T_{323}T_{101}^* e^{i(\delta_3-\delta_1)}) - \frac{1}{2450}\Im(T_{343}T_{321}^* e^{i(\delta_3-\delta_1)})$$
$$- \frac{17}{5^2 3^2 56}\Im(T_{343}T_{121}^* e^{i(\delta_3-\delta_1)}) - \frac{13}{1400}\Im(T_{323}T_{101}^* e^{i(\delta_3-\delta_1)}) - \frac{1}{2450}\Im(T_{343}T_{321}^* e^{i(\delta_3-\delta_1)})$$
$$- \frac{17}{5^2 3^2 56}\Im(T_{343}T_{121}^* e^{i(\delta_3-\delta_1)}) - \frac{1}{63}\Im(T_{343}T_{101}^* e^{i(\delta_3-\delta_1)}) - \frac{1}{600}\Im(T_{123}T_{121}^* e^{i(\delta_3-\delta_1)})$$
$$\left. - \frac{1}{75}\Im(T_{123}T_{101}^* e^{i(\delta_3-\delta_1)})\right\}$$

$$B_{4,3d} = \cos^2 2\zeta \sin 2\zeta \left\{ \frac{23}{7840} \Im(T_{323}T_{343}^*) + \frac{11}{7840} \Im(T_{323}T_{123}^*) + \frac{3}{560} \Im(T_{343}T_{123}^*) \right.$$
$$+ \frac{53}{7840} \Im(T_{345}T_{323}^* e^{i(\delta_5-\delta_3)}) + \frac{9}{1372} \Im(T_{345}T_{343}^* e^{i(\delta_5-\delta_3)}) + \frac{37}{3840} \Im(e^{i(\delta_5-\delta_3)} T_{345}T_{123}^*)$$
$$- \frac{23}{1120} \Im(e^{i(\delta_5-\delta_1)} T_{345}T_{321}^*) + \frac{29}{1440} \Im(T_{345}T_{121}^* e^{i(\delta_5-\delta_1)}) - \frac{5}{288} \Im(T_{345}T_{101}^* e^{i(\delta_5-\delta_1)})$$
$$- \frac{3}{7^2 5^2 16} \Im(T_{323}T_{321}^* e^{i(\delta_3-\delta_1)}) + \frac{1}{700} \Im(T_{323}T_{121}^* e^{i(\delta_3-\delta_1)}) + \frac{1}{80} \Im(T_{323}T_{101}^* e^{i(\delta_3-\delta_1)})$$
$$+ \frac{1}{1960} \Im(T_{343}T_{321}^* e^{i(\delta_3-\delta_1)}) + \frac{11}{5040} \Im(T_{343}T_{121}^* e^{i(\delta_3-\delta_1)}) + \frac{1}{72} \Im(T_{343}T_{101}^* e^{i(\delta_3-\delta_1)})$$
$$\left. - \frac{11}{5600} \Im(T_{123}T_{321}^* e^{i(\delta_3-\delta_1)}) - \frac{1}{2400} \Im(T_{123}T_{121}^* e^{i(\delta_3-\delta_1)}) + \frac{1}{96} \Im(T_{123}T_{101}^* e^{i(\delta_3-\delta_1)}) \right\} \quad (12)$$

The sixteen needed relevant transition matrix elements $T_{\lambda_1\lambda_2 L}$ that appear in Eqs.(10), (11) and (12) have been derived by several authors : using either the Coulomb Green's functions sturmians expansion (Maquet, 1977) or the Dalgarno - Lewis method in a closed integral form Radhakrishnan and Thayyullathil (2004). As announced in the introduction, we use here the implicit summation technique by Faye et al. (2010) used very recently for 1s,2s,3s, 2p and 3p initial states, in the case of linearly and circularly polarized light, at wavelength comprising between the two and the three photon thresholds ionization.

3. THE χ AND δ ASYMMETRIC TERMS

It appears that the elliptic dichroic effects can be observed in the ($B_{2,ns}$, $B_{4,ns}$), ($B_{2,np}$, $B_{4,np}$), and ($B_{2,3d}$, $B_{4,3d}$), asymmetric terms of Eqs.(8), (10) and (12),respectively ,in a compact form. As ζ in Eq(2),depends on both χ and δ parameters, one can obtain now the difference between the left and right polarized light in two ways as shown by Faye and Wane (2011).

The first one depending on the elliptic angle χ named $D_\zeta^{\pm\chi}$, at fixed value of the δ phase lag, defined as:

$$D_\zeta^{\pm\chi} = \frac{1}{I^2} \frac{d\sigma_{nl}}{d\Omega}(+\chi,\delta) - \frac{1}{I^2} \frac{d\sigma_{nl}}{d\Omega}(-\chi,\delta) \quad (13)$$

Or usually as:

$$R = \frac{D_\zeta^{\pm\chi}}{\frac{1}{I^2} \frac{d\sigma_{nl}}{d\Omega}(+\chi,\delta) + \frac{1}{I^2} \frac{d\sigma_{nl}}{d\Omega}(-\chi,\delta)}$$

The second one depending on the phase lag (lead) δ: $D_\zeta^{\pm\delta}$,with:

$$D_\zeta^{\pm\delta} = \frac{1}{I^2} \frac{d\sigma_{nl}}{d\Omega}(\chi,+\delta) - \frac{1}{I^2} \frac{d\sigma_{nl}}{d\Omega}(\chi,-\delta) \quad (14)$$

usually as

$$R = \frac{D_\zeta^{\pm\delta}}{\frac{1}{I^2}\frac{d\sigma_{nl}}{d\Omega}(\chi,+\delta) + \frac{1}{I^2}\frac{d\sigma_{nl}}{d\Omega}(\chi,-\delta)}$$

The above equations show that the analytical expressions of $D_\zeta^{\pm\chi}$ or $D_\zeta^{\pm\delta}$ are related either to the couples ($B_{2,ns}$, $B_{4,ns}$) of Eq.(8), ($B_{2,np}$, $B_{4,np}$) of Eq.(10), and ($B_{2,3d}$, $B_{4,3d}$) of Eq. (12). The general form of R is given by:

$$R(\phi) = \frac{B_2 \sin 2\phi + B_4 \sin 4\phi}{A_0 + A_2 \cos 2\phi + A_4 \cos 4\phi + A_6 \cos 6\phi} \qquad (14')$$

In these expressions the occurrence of the imaginary part of the interference terms associated with the different paths leading to the final states, reflects their strong dependence on the incoming photons, i.e., with the ionization process. But, in the case treated here, we limit ourselves to photons with energies comprising between the two and three photon threshold ionization. Then the radial transition matrix elements $T_{\lambda_1\lambda_2 L}$ are real. In ($B_{2,ns}$, $B_{4,ns}$), ($B_{2,np}$, $B_{4,np}$), and ($B_{2,3d}$, $B_{4,3d}$) all the interference terms corresponding to the same final orbital momentum L vanish. Then the difference $D_\zeta^{\pm\chi}$ or $D_\zeta^{\pm\delta}$ can be obtained explicitly for each state as follow:

3.1 *l=0* Initial States

From Eqs. (2),(9),(13) or (14), one gets:

$$D_\zeta^{\pm\delta} = 2(B_{2,ns}\sin 2\phi + B_{4,ns}\sin 4\phi) = \beta tg\chi \sin\delta \sin(\delta_3 - \delta_1)(b_{2,ns}\sin 2\phi + b_{4,ns}\cos 2\zeta \sin 4\phi) \qquad (15)$$

with:

$$\beta = \frac{2(1 - tg^2\chi \sin^2\delta)}{(1 + tg^2\chi \sin^2\delta)^2}$$

$$D_\zeta^{\pm\chi} = 2(B_{2,ns}\sin 2\phi + B_{4,ns}\sin 4\phi) \qquad (15')$$

Has the same form as Eq.(15)

3.2 *l*=1 Initial States

Eq.(2),(11) and (13) or (14), give:

$$D_\zeta^{\pm\delta} = 2(B_{2,np}\sin 2\phi + B_{4,np}\sin 4\phi) = \beta tg\chi \sin\delta \{b_{2,np}\sin 2\phi + b_{4,np}\cos 2\zeta \sin 4\phi\} \qquad (16)$$

or

$$D_{\zeta}^{\pm\chi} = 2(B_{2,np}\sin 2\phi + B_{4,np}\sin 4\phi) \quad (16')$$

has the same form as Eq.(16).

3.3 *l=2* Initial States

From Eqs.(2),(12) and (13) or (14), one obtains:

$$D_{\zeta}^{\pm\delta} = 2(B_{2,3d}\sin 2\phi + B_{4,3d}\sin 4\phi) = \beta tg\chi \sin\delta\left\{b_{2,3d}\sin 2\phi + b_{4,3d}\cos 2\zeta \sin 4\phi\right\} \quad (17)$$

or

$$D_{\zeta}^{\pm\chi} = 2(B_{2,3d}\sin 2\phi + B_{4,3d}\sin 4\phi) \quad (17')$$

has the same form as Eq.(17)

The terms ($b_{2,ns}$, $b_{4,ns}$) contain only the real transition matrix elements, whereas ($b_{2,np}$, $b_{4,np}$) and ($b_{2,3d}$, $b_{4,3d}$) are combinations of the sine of the phase shifts difference of the continua. We give them in the appendix.

Furthermore, it appears from Eq.(15), if: $\delta = \delta_3 - \delta_1$, by using the properties of the Γ function appearing in the Coulomb phase shift, (Faye and Wane, 2011), that the energies of the photoelectron are directly related to the phase lag as:

$$tg\delta = \frac{5k_e}{1-6k_e^2} \quad (18)$$

the same form has been obtained by Faye and Wane (2011) for hydrogen atom initially in its 3p excited state.

Thus if $\chi = \pi/4$, the analytical expression for the dichroic term $D_{\zeta}^{\pm\delta}$ from Eq.(15) is given by:

$$D_{\zeta}^{\pm\delta} = \frac{2(1-\sin^2(\delta_3-\delta_1))}{(1+\sin^2(\delta_3-\delta_1))^2}\sin^2(\delta_3-\delta_1)b_{2,ns}(\sin 2\phi + \cos 2\zeta \sin 4\phi) \quad (19)$$

One notes that the quadratic form of the sine of the phase shift difference of Eq.(19) is not possible for the np of Eq.(16) and 3d of Eq.(17) cases, due to the presence of three and two different Coulomb phase shifts in the couples($b_{2,np}$ $b_{4,np}$) and ($b_{2,3d}$ $b_{4,3d}$) (Appendix) for which it is not possible to find a single phase δ that is equal to all three or two phase shifts at the same time. Although these results have been established for hydrogen, Eq.(18) is general and should apply to the case of complex atoms with suitable modification of the kinetic energy. Eq.(19) describes an isolation equation of the phase shift through the phase δ, e.g. if $\delta \to 0$ (i.e. for small values of the phase), to first order with respect to δ, $\sin\delta \approx \delta$ and $\cos\zeta \approx 1$, as a consequence: Eq.(2)shows that the three photons are nearly linearly polarized along the semimajor axis, Eq.(19) behaves as:

$$D_{\zeta}^{\pm\delta\to 0} \approx 2\delta^2 b_{2,ns}(1+2\cos 2\phi)\sin 2\phi \quad (19')$$

which is nonzero, although its value is relatively very weak; on the other side,

$tg\delta \approx \delta$ from which it follows from Eq.(18) ($6k_e^2 << 1$) that: $k_e \approx \frac{\delta}{5}$.

This small value of the photoelectron energy corresponds to the near threshold ionization within the first Born approximation (Bethe and Salpeter, 1957).

The applications of Eqs.(19)and (19') displayed in Fig.(1), exhibit a left handed photoelectron distribution in the cases where $\delta = \delta_3 - \delta_1$ and $\delta = 10^{-3}$ rad, respectively. Recently, using linearly polarized light, Ricz,S. et al.(2007) have observed a surprisingly nonzero left-right asymmetry in noble gases.

4. NUMERICAL RESULTS AND DISCUSSION

We restrict ourselves on the ζ dependence as shown in Eq.(2).

4.1 The Fundamental State

Table 1 shows for λ=250 nm, some numerical values of the angular coefficients $A_{0,1s}$, $A_{2,1s}$ $A_{4,1s}$, $A_{6,1s}$, $B_{2,1s}$ and $B_{4,1s}$ calculated for a given ζ. The coefficient $B_{2,1s}$ is positive only for $\zeta=50^0$ and 60^0 whereas $B_{4,1s}$ is always negative. These coefficients have the same magnitude as $A_{0,1s}$. The smallest contribution is noted for the $A_{6,1s}$ at $\zeta= 20^0$, 40^0 and 50^0. These values can be understood if one refers to the lack of the interference terms contributions in its expression; that is not the case for $\zeta=60^0$ where it is superior to the value of $A_{4,1s}$ for which the first quadratic term appearing in $A_{4,1s}$ Eq.(9) and related to channel 1/ of subsect.**2.1**, contributes destructively.

Table 1. Three photon ionization (λ=250 nm): numerical values of the angular coefficients $A_{0,1s}$, $A_{2,1s}$, $A_{4,1s}$,$A_{6,1s}$, $B_{2,1s}$ and $B_{4,1s}$, in cm^6/W^2sterad, as a function of the ellipticity parameter ζ, for Hydrogen atom initially in its fundamental state H(1s).The format A(n) means $A\times10^n$

Angular coefficients	$\zeta=20^0$	$\zeta=30^0$	$\zeta=40^0$	$\zeta=50^0$	$\zeta=60^0$
$A_{0,1s}$	2.2893(-47)	1.3722(-47)	7.7348(-48)	7.7348(-48)	1.372(-47)
$A_{2,1s}$	1.8569(-47)	6.0233(-48)	8.203(-49)	-1.0739(-48)	-8.1246(-48)
$A_{4,1s}$	1.2505(-48)	5.3292(-49)	6.4274(-50)	6.425(-50)	5.3269(-49)
$A_{6,1s}$	8.081(-51)	2.1619(-49)	9.0516(-51)	-9.0516(-51)	-2.3554(-48)
$B_{2,1s}$	-7.2974(-48)	-6.4179(-48)	-2.5339(-48)	2.5244(-48)	6.4155(-48)
$B_{4,1s}$	-5.5907(-48)	-3.2090(-48)	-4.3998(-49)	-4.3998(-49)	-3.2090(-48)

Fig.1, shows $I(\phi)$, the PAD in polar coordinates, and the corresponding elliptic dichroic (ED)signal $R(\phi)$, in Cartesian plots. The results are given for three values of ζ: 20^0, 40^0 and 60^0. In addition, the special case for which $\chi=45^0$ and $\delta = \delta_3 - \delta_1$ has also been considered.

A two lobed PAD is noted for $\zeta=20^0$ with maxima directed along $\phi=165^0$ (345^0}); for $\zeta=40^0$ the distribution is nearly isotropic while for $\zeta=60^0$ it is stretched along the direction of $\phi=67.5^0(247.5^0)$. An isotropic PAD is obtained for the special case where $\zeta=43.83^0$ ($\chi=45^0$ and $\delta=\delta_3-\delta_1$). A two lobed shape directed along $\phi=90^0(270^0)$ is obtained for $\zeta=10^{-3}$rad ($\chi=45^0$, $\delta=10^{-3}$rad). One can explain the isotropic shapes for $\zeta=40^0$ and $\zeta=43.83^0$, from the relatively strong isotropic term $A_{0,1s}$ which is not sensitively modified by the others terms. For $\zeta=10^{-3}$

rad, the minima noted at $\phi=0^0(180^0)$ can be explained by the strongly destructive contributions of the $A_{2,1s}$}and $A_{4,1s}$} to the PAD.

The corresponding ED signals for $\zeta=40^0$, show two maxima at $\phi=135^0(315^0)$ and two minima at $\phi=37.5^0(217.5^0)$; while for $\zeta=60^0$ they are at $\phi=52.5^0(232.5^0)$ and $\phi=127.5^0(307.5^0)$;it is notable that the ED for $\zeta=20^0$ shows four maxima at $\phi=75^0$; 142^0; 255^0 and 322.5^0 and four minima at$\phi=37.5^0$;105^0; 210^0 and 285^0. The strongest signal obtained with $\zeta=60^0$ comes from the destructive contributions of the coefficients $A_{2,1s}$ and $A_{6,1s}$ .These negative values would come from the positive role played by the interference between the channels : 1/2,1/3 and 2/3,in subsection **2.1**.The ED signal for $\zeta=43.83^0$(corresponding to nearly circularly polarized light $\zeta=45^0$) which we have amplified by 5, exhibits maxima at $\phi=45^0(225^0)$ and minima at $\phi=135^0(315^0)$.In addition, for $\zeta=10^{-3}$rad($\chi=45^0$,$\delta=10^{-3}$ rad),for which the photons are nearly linearly polarized along the semimajor axis, we have amplified the dichroic signal by 3. 10^4 to allow the observation of the positions of the two maxima at $\phi=4^0(180^0)$ and minima at $\phi=180^0(356^0)$.

4.2 The 2s and 2p Excited States

Table 2, in a way similar to Table 1 gives for λ=860 nm, the angular coefficients for: (a) the $A_{0,2s}$, $A_{2,2s}$, $A_{4,2s}$, $A_{6,2s}$, $B_{2,2s}$ and $B_{4,2s}$ of the 2s excited state; and (b), the $A_{0,2p}$, $A_{2,2p}$, $A_{4,2p}$, $A_{6,2p}$, $B_{2,2p}$ and $B_{4,2p}$ of the 2p excited state. For case (a), the $B_{4,2p}$ takes always positive values while the $B_{2,2s}$ takes negative values for $\zeta=50^0$ and 60^0. These negative values come from the fact that the destructive interference term between channels 1/2 is strongest than that constructive between channels 1/3.On the other hand, the $B_{4,2s}$ values are inferior to that of $B_{2,2s}$, regardless the value of the ζ.The smallest value of the coefficients is obtained for $A_{6,2s}$ for $\zeta=40^0$ and 50^0.

For case (b),the $B_{4,2p}$ takes always positive values as in (a) while the $B_{2,2p}$ takes negative values for $\zeta=20^0$, 30^0 and 40^0. These negative values can be understood from Eq.(11) where among the eleven interference terms, between channels of final orbital momenta, L=4,L=2;L=4,L=0;and L=2,L=0;five of them with the maximum,(between channels 3/6 of subsect.**2.2**) give destructive contributions. On the other hand, the positive values of the $B_{4,2p}$ come from the two strongest constructive interference terms between channels 1/3 and 1/6. The smallest value of the coefficients is obtained for $A_{6,2p}$ for $\zeta=40^0$ and 50^0.We note that, regardless the values of ζ, the contributions of the ($B_{2,2p}$,$B_{4,2p}$) to the PAD are strongest than ($B_{2,2s}$,$B_{4,2s}$).

In Fig 2 as in fig 1, we present the PAD :(a), for 2s and (b)for 2p, excited states. In fig 2(a): for $\zeta=20^0$,a two marked lobes directed along the y- semiminor axis is noted, while for $\zeta=40^0$,a isotropic shape is obtained; for $\zeta=60^0$, the two maxima are directed along the x-semimajor axis, with a shallow minimum noted along the y-semiminor axis. These shapes can be explained if one refers to the PAD of Eq.(8), and replaces ϕ by zero.

One sees that for $\zeta=20^0$ the negative contributions of both $A_{2,2s}$ and $A_{4,2s}$, lead to a low minimum; while for $\zeta=60^0$,the maxima come from the strong positive contributions of $A_{0,2s}$ and $A_{2,2s}$ which cancel the negative contributions of $A_{4,2s}$ and $A_{6,2s}$. On the other hand, the isotropic shape comes from the isotropic term $A_{0,2s}$ which is relatively not modified by the others terms.

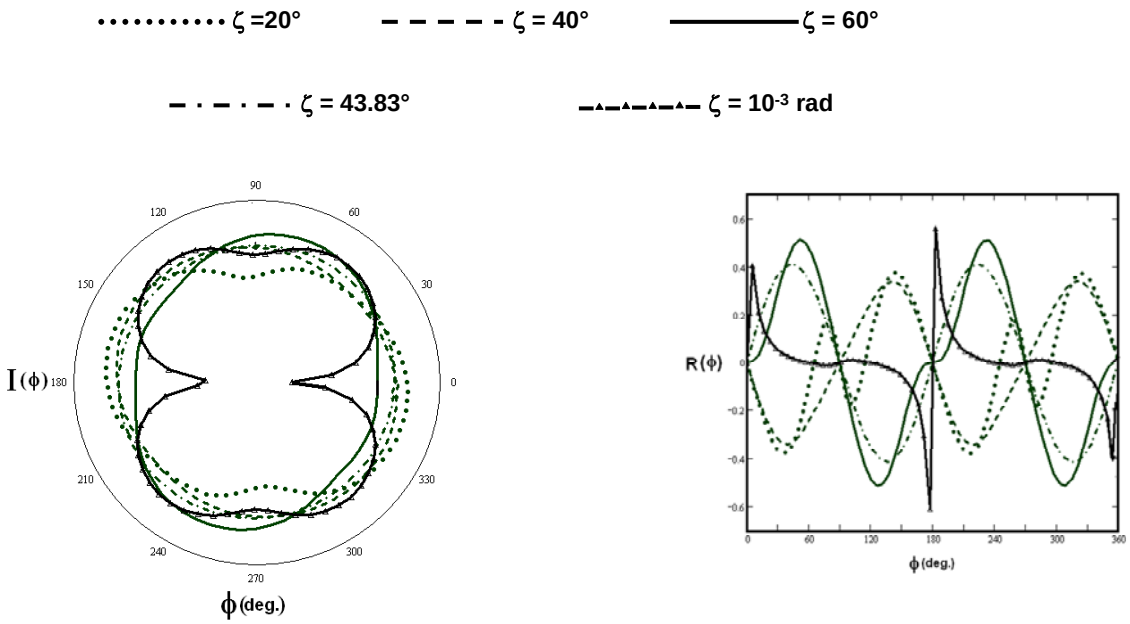

Fig. 1. Three photon ionization (λ=250 nm) of H(1s) with elliptically polarized light defined by varying the ellipticity ζ: ϕ-dependence of the photoelectron angular distribution (PAD), I(ϕ) in polar diagram, and the corresponding elliptic dichroic (ED) signal R(ϕ) in Cartesian plots.

Full circles, $\zeta=20^0$; dashed line, $\zeta=40^0$; solid line, $\zeta=60^0$; Chain lines, $\zeta=43.83^0$($\chi=45^0$ and $\delta=\delta_3 - \delta_1$), R($\phi$) has been multiplied by 5; Triangles line, $\zeta=10^{-3}$rad ($\chi=45^0$ and $\delta=10^{-3}$rad),the amplitude has been multiplied by 3.10^4.

Table 2. Same as in Table 1, but for λ=860 nm: (a) for H(2s) and (b) for H(2p), where the second subscript appearing in each coefficient is replaced by 2s and 2p respectively

a)	**$\zeta=20^0$**	**$\zeta=30^0$**	**$\zeta=40^0$**	**$\zeta=50^0$**	**$\zeta=60^0$**
$A_{0,2s}$	5.3441(-43)	6.7922(-43)	7.7381(-43)	7.7381(-43)	6.7929(-42)
$A_{2,2s}$	-2.9695(-43)	-2.5522(-43)	-1.046(-43)	1.0916(-43)	2.9460(-43)
$A_{4,2s}$	-1.8330(-43)	-7.8141(-44)	-9.4170(-45)	-9.4170(-45)	-7.8072(-44)
$A_{6,2s}$	8.8435(-44)	2.4596(-44)	1.0301(-45)	-1.0301(-45)	-2.4589(-44)
$B_{2,2s}$	7.7312(-44)	7.2821(-44)	2.8769(-44)	-2.8769(-44)	-7.2821(-44)
$B_{4,2s}$	6.3487(-44)	3.6431(-44)	4.9959(-45)	4.9959(-45)	3.6424(-44)

b)	**$\zeta=20^0$**	**$\zeta=30^0$**	**$\zeta=40^0$**	**$\zeta=50^0$**	**$\zeta=60^0$**
$A_{0,2p}$	7.6483(-43)	1.3940(-42)	5.085(-43)	5.6354(-43)	1.3936(-42)
$A_{2,2p}$	-3.6272(-44)	8.7438(-43)	-3.3762(-44)	-6.5336(-44)	-8.7406(-43)
$A_{4,2p}$	-4.3481(-44)	5.1703(-45)	-2.2341(-45)	4.6175(-46)	5.1864(-45)
$A_{6,2p}$	-1.5957(-44)	-5.2978(-45)	-1.8590(-46)	1.6427(-46)	5.3134(-45)
$B_{2,2p}$	-8.1204(-44)	-7.3719(-43)	-2.8212(-44)	2.9110(-43)	7.3719(-43)
$B_{4,2p}$	2.8718(-43)	2.3606 (-43)	2.2613(-44)	3.238(-44)	2.7751(-43)

The corresponding ED signals exhibit: two maxima: at $\phi=15^0(195^0)$ for $\zeta=20^0$; at $\phi=30^0(210^0)$ for $\zeta=40^0$, and at $\phi=112.5^0(192.5^0)$ for $\zeta=60^0$;and two minima: located at $\phi=165^0(345^0)$; $\phi=150^0(330^0)$ and $\phi=67.5^0(247.5^0)$ respectively. However, the amplitude corresponding to $\zeta=40^0$ has been multiplied by 10.This low amplitude is the consequence of the relatively small contributing asymmetric terms $B_{2,2s}$, $B_{4,2s}$. In fig 2(b), a four lobed PAD is obtained for $\zeta=20^0$ with two shallow minima at $\phi=67.5^0(247.5^0)$ and $\phi=165^0(345^0)$; a truncated isotropic distribution for $\zeta=40^0$, while for $\zeta=60^0$,the PAD shows a two marked lobes pointing along $\phi=60^0(240^0)$.The shallow minima exhibited for $\zeta=20^0$, are due: for $\phi=67.5^0(247.5^0)$,to the destructive asymmetric terms $B_{2,2p}$, $B_{4,2p}$, associated with the negative $A_{6,2p}$ term ,which lower the constructive terms $A_{0,2p}$ and $A_{2,2p}$; for $\phi=165^0(345^0)$, to the negative asymmetric term $B_{4,2p}$ associated with the destructive terms $A_{2,2p}$,$A_{4,2p}$,which lower the positive values of $B_{2,2p}$,$A_{0,2p}$. As to $\zeta=60^0$,the maxima obtained for $\phi=60^0$,would come from the combination of the constructive terms $A_{0,2p}$, $A_{2,2p}$ and $A_{4,2p}$ which cancel the negative ones $A_{6,2p}$, $B_{2,2p}$ and $B_{4,2p}$.The truncated isotropic distribution is due to the relatively high contribution of the isotropic term $A_{0,2p}$.

The corresponding ED signals exhibit: for $\zeta=20^0$ as well for $\zeta=40^0$, which have been amplified by 3 and 10, respectively, four maxima located at $\phi=15^0(112.5^0)$,$\phi=195^0(292.5^0)$ and $\phi=15^0(120^0)$, $\phi=195^0(300^0)$,respectively; four minima at $\phi=60^0(165^0)$, $\phi=240^0(345^0)$;and $\phi=60^0(165^0)$, $\phi=240^0(345^0)$;respectively. While for $\zeta=60^0$, the signal shows two maxima at $\phi=22.5^0(202.5^0)$ and two minima at $\phi=157.5^0(337.5^0)$.The highest ED amplitude displayed for $\zeta=60^0$,is obtained owing to the combination of the strong asymmetric contributions of $B_{2,2p}$ and $B_{4,2p}$ associated to destructive $A_{2,2p}$ term.

4.3 The 3s, 3p and 3d, Excited States

Table 3, in a way similar to Table 1 gives for λ=2420 nm, the angular coefficients for: (a),the $A_{0,3s}$, $A_{2,3s}$, $A_{4,3s}$, $A_{6,3s}$,$B_{2,3s}$ and $B_{4,3s}$ of the 3s state;(b), the $A_{0,3p}$, $A_{2,3p}$, $A_{4,3p}$, $A_{6,3p}$,$B_{2,3p}$ and $B_{4,3p}$ of the 3p state and (c),the $A_{0,3d}$, $A_{2,3d}$, $A_{4,3d}$, $A_{6,3d}$,$B_{2,3d}$ and $B_{4,3d}$ of the 3d state.

For case (a), the $B_{4,3s}$} takes always positive values while the $B_{2,3s}$ takes negative values for $\zeta=50^0$ and 60^0. These positive and negative values can be understood from the constructive interference term between channels 1/2 which is over the destructive one between channels 1/3 subsect.**2.3**. On the other hand, the $B_{4,3s}$ values are inferior to that of $B_{2,3s}$,regardless the values of ζ .The smallest value of the coefficients is obtained for $A_{6,3s}$ for $\zeta=40^0$ and 50^0.

In case (b),the $B_{2,3p}$ takes negative values only for $\zeta=50^0$ and 60^0 while $B_{4,3p}$ takes always negative values .These obtained signs, for $B_{2,3p}$ are the result of the two constructive interference between channels 1/4 and between channels 1/6, associated to all the others destructive ones. The same remark holds for $B_{4,3p}$. $B_{2,3p}$ is stronger than $B_{4,3p}$ regardless the value of the ζ ,and a great difference between them is noted for $\zeta=50^0$.

For case (c), the $B_{2,3d}$ takes positive values only for $\zeta=50^0$ and 60^0 while $B_{4,3d}$ takes always positive values. As in case (b), the $B_{2,3d}$ values are stronger than $B_{4,3d}$ values; great differences are noted between them for $\zeta=40^0$ and $\zeta=50^0$.These signs can be explained if one considers Eq.(12),where in $B_{2,3d}$, the seven destructive terms with the strongest interference between channels subsection **2.3**, 1/3, 1/2, 1/4 and 2/6, are over the seven constructive ones. The situation is inverted for $B_{4,3d}$, where the nine positive terms are over the six negative ones.

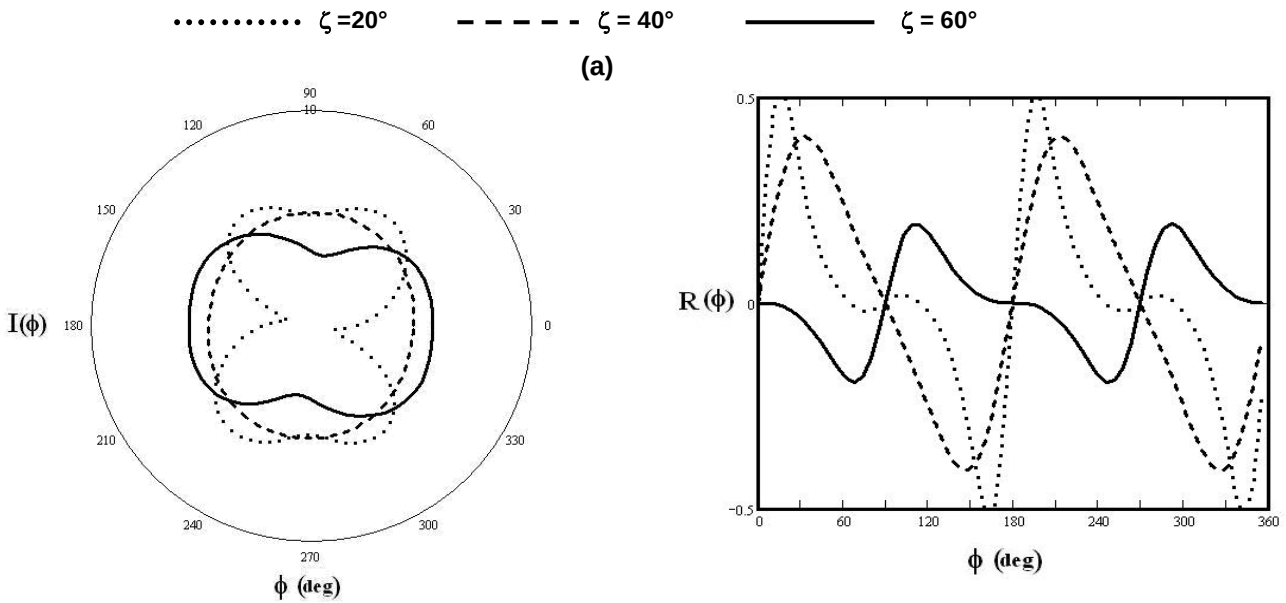
ζ =20°
ζ = 40°
ζ = 60°
(a)
I(ϕ)
ϕ (deg)
R (ϕ)
ϕ (deg)

(b)

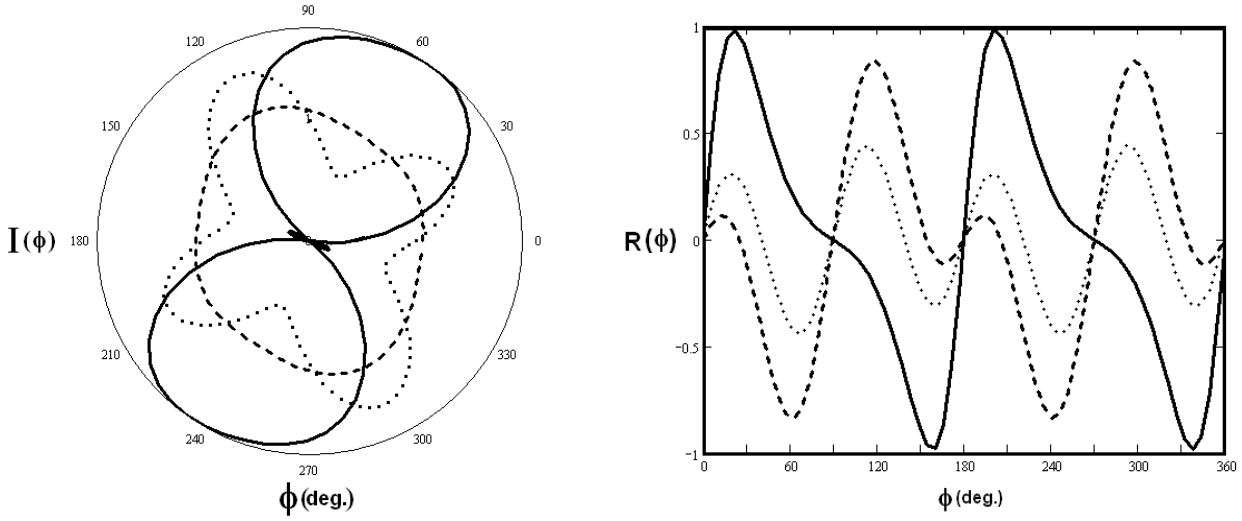

Fig. 2. The same as in Fig 1 for the first three curves, but λ=860 nm: (a) for H(2s) and (b) for H(2p); the corresponding amplitudes for ζ=40^0 have been multiplied by 10 in (a) and (b)

In fig 3 as in fig 2, shows the PAD for: (a), 3s; (b),3p; and (c),3d; excited states. The PAD in fig 3(a), shows for $\zeta=20^0$ two marked lobes along the y-semiminor axis with shallow minima; for $\zeta=40^0$ a two lobed shape is also obtained in the same direction, but a nonzero minimum is noted for the semimajor axis. For $\zeta=60^0$ the distribution shows a pronounced two lobes shape directed along the x-semimajor axis.

The nearly zero minima noted for $\zeta=20^0$ are the result of the $A_{2,3s}$, $A_{4,3s}$ negative contributions, which nearly sweep the isotropic term ; for $\zeta=40^0$, the isotropic term is less affected by the same negative terms, which leads, as a consequence to shallow minima; for $\zeta=60^0$ the $A_{2,3s}$ now contributes positively to the PAD, while $A_{4,3s}$ is always negative, but, not enough strong to modify the constructive terms; finally the maxima occur along the semimajor axis.

All the corresponding ED signals exhibit, for $\zeta=20^0$,40^0 and 60^0 two maxima located at: $\phi=7.5^0(187.5^0)$; $30^0(210^0)$ and $\phi=97.5^0(277.5^0)$, respectively; two minima at $\phi=172.5^0(352.5^0)$,$150^0(330^0)$ and $\phi=82.5^0(262^0)$.We have multiplied by 10 the ED signal for $\zeta=40^0$to allow the observation of this low signal.

In fig 3(b), the PAD shows two lobed shape for $\zeta=20^0$ and 60^0,aligned towards the x-semimajor and nearly the y-semiminor axes, respectively; whereas for $\zeta=40^0$ a truncated isotropic distribution is observed. If $\phi=0$, one can note that, the maxima observed for $\zeta=20^0$ are due to the strong positive contributions of the $A_{0,3p}$,$A_{2,3p}$ and $A_{4,3p}$, to the PAD; that is not the case for $\zeta=60^0$ where only the $A_{4,3p}$ subsists; as a consequence, nearly zero minima occur.

The corresponding ED signals exhibit for $\zeta=40^0$ and 60^0 two maxima at $\phi=45^0225^0$ and $\phi=165^0(345^0)$ and two minima located at $\phi=135^0(315^0)$ and $\phi=15^0$ (195^0), respectively; the same situation is observed for $\zeta=20^0$ where the strongest ED signal shows two maxima at $\phi=60^0(240^0)$ and two minima positioned at $\phi=112.5^0(292.5^0)$. But, we have amplified by 10 the corresponding amplitude for $\zeta=40^0$.The observed strong ED for $\zeta=20^0$, comes from both to the positive contributions of the asymmetric terms $B_{2,3p}$, $B_{4,3p}$ and the presence of the two negative terms $A_{2,3p}$,$A_{4,3p}$.

In fig 3(c), the PAD displays two isotropic shapes for $\zeta=20^0$ and 60^0 whereas for $\zeta=40^0$, it shows a two lobes shape directed towards $\phi=120^0(300^0)$ with shallow minima at $\phi=15^0(195^0)$.These isotropic shapes are due to the strong value of the contributing isotropic term, which is less affected by the others positive or negative terms of the PAD. For $\zeta=40^0$, all the six terms of the PAD, contribute positively to give the maxima noted in that direction.

The corresponding ED signals exhibit for $\zeta=20^0$,40^0 and 60^0, two maxima located at $\phi=135^0(345^0)$; $\phi=150^0(330^0)$ and $\phi=45^0(225^0)$; and two minima at $\phi=45^0(225^0)$; $\phi=30^0(210^0$ and $\phi=135^0(315^0)$, respectively. We have multiplied by 3 the low ED signals corresponding to $\zeta=20^0$ and 60^0. The strongest signal for $\zeta=40^0$, is the result of the strong contribution of the $B_{2,3d}$ coefficient.

Table 3. Same as in Table 1, but for λ=2420 nm : (a) for H(3s) , (b) for H(3p) and (c) for H(3d), where the second subscript occurring in each coefficient is replaced by 3s, 3p and 3d, respectively

a)	**ζ=20^0**	**ζ=30^0**	**ζ=40^0**	**ζ=50^0**	**ζ=60^0**
$A_{0,3s}$	2.2291(-41)	1.8115(-41)	1.539(-41)	1.539(-41)	1.8115(-41)
$A_{2,3s}$	-1.1223(-41)	-1.3660(-41)	-5.973(-42)	6.8224(-42)	2.070(-41)
$A_{4,3s}$	-1.0908(-41)	-4.6473(-42)	-5.6048(-43)	-5.5048(-43)	-4.6473(-42)
$A_{6,3s}$	1.6873(-42)	4.6940(-43)	1.9655(-44)	-1.9655(-44)	-4.6915(-43)
$B_{2,3s}$	1.5358(-42)	1.3507(-42)	5.3347(-43)	-5.3347(-43)	-1.3505(-42)
$B_{4,3s}$	1.1764(-42)	6.7537(-43)	9.2627(-44)	9.2627(-44)	6.7537(-43)

b)	**ζ=20^0**	**ζ=30^0**	**ζ=40^0**	**ζ=50^0**	**ζ=60^0**
$A_{0,3p}$	3.0584(-39)	3.5887(-39)	1.0361(-39)	1.2121(-39)	3.5879(-39)
$A_{2,3p}$	3.9769(-39)	3.5920(-39)	1.2260(-40)	-7.3222(-40)	-3.5911(-39)
$A_{4,3p}$	1.4412(-39)	5.0004(-40)	7.4049(-41)	6.0292(-41)	4.9988(-40)
$A_{6,3p}$	-2.239(-41)	2.6001(-42)	-2.6041(-43)	-1.0885(-43)	-2.3554(-42)
$B_{2,3p}$	2.1884(-480)	1.0656(-39)	7.5988(-41)	-4.2066(-40)	-1.0656(-39)
$B_{4,3p}$	-5.3270(-41)	-5.6854(-41)	-4.1935(-42)	-7.7961(-42)	-5.6838(-41)

c)	**ζ=20^0**	**ζ=30^0**	**ζ=40^0**	**ζ=50^0**	**ζ=60^0**
$A_{0,3d}$	4.0508(-40)	1.7426(-40)	3.7679(-41)	3.2588(-41)	1.7421(-40)
$A_{2,3d}$	-2.8424(-41)	6.1915(-42)	-8.2292(-42)	4.5766(-43)	2.6342(-42)
$A_{4,3d}$	-1.6026(-41)	-1.7671(-42)	7.3994(-43)	-2.1309(-43)	-1.7666(-42)
$A_{6,3d}$	6.3585(-43)	2.425(-43)	-1.691(-45)	-1.0154(-44)	-2.4241(-43)
$B_{2,3d}$	-4.8688(-41)	-1.6537(-41)	-2.5339(-41)	6.5303(-42)	1.6537(-41)
$B_{4,3d}$	2.8458(-42)	5.946(-43)	2.2399(-43)	8.1555(-44)	5.946(-43)

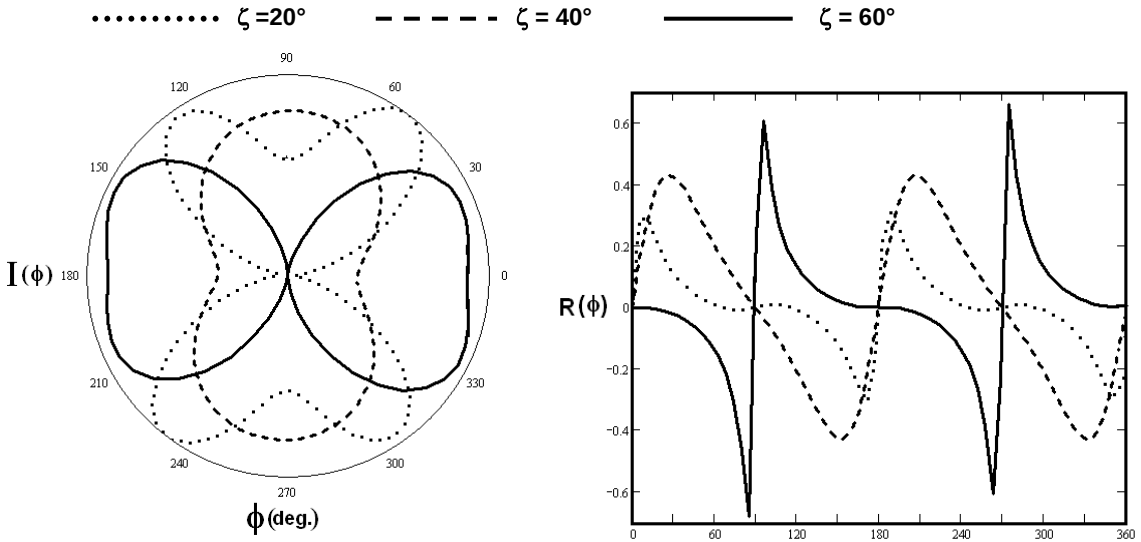

(a)

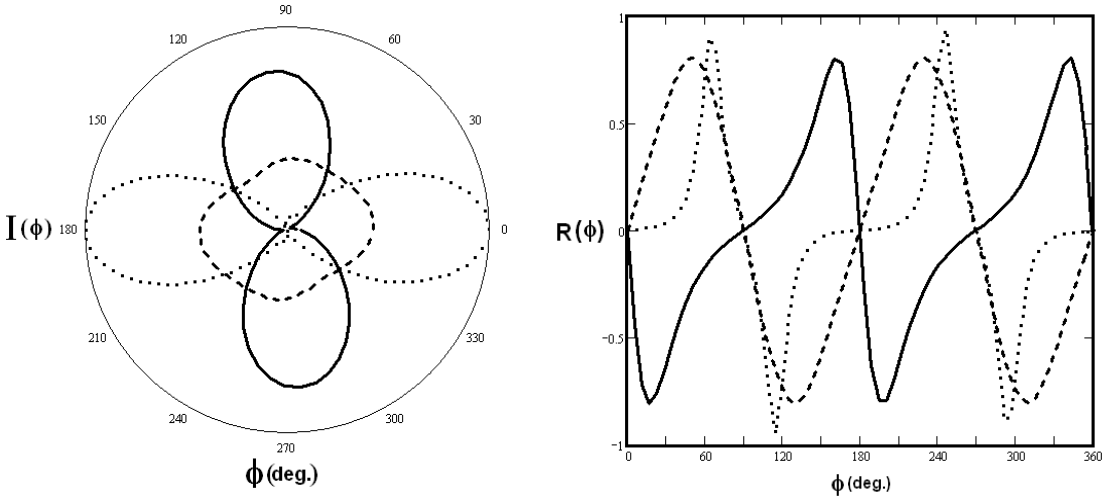
90
120
60
150
30
I(ϕ)
180
0
210
330
240
300
270
ϕ(deg.)
1
0.5
R(ϕ)
0
−0.5
−1
0
60
120
180
240
300
360
ϕ(deg.)

(b)

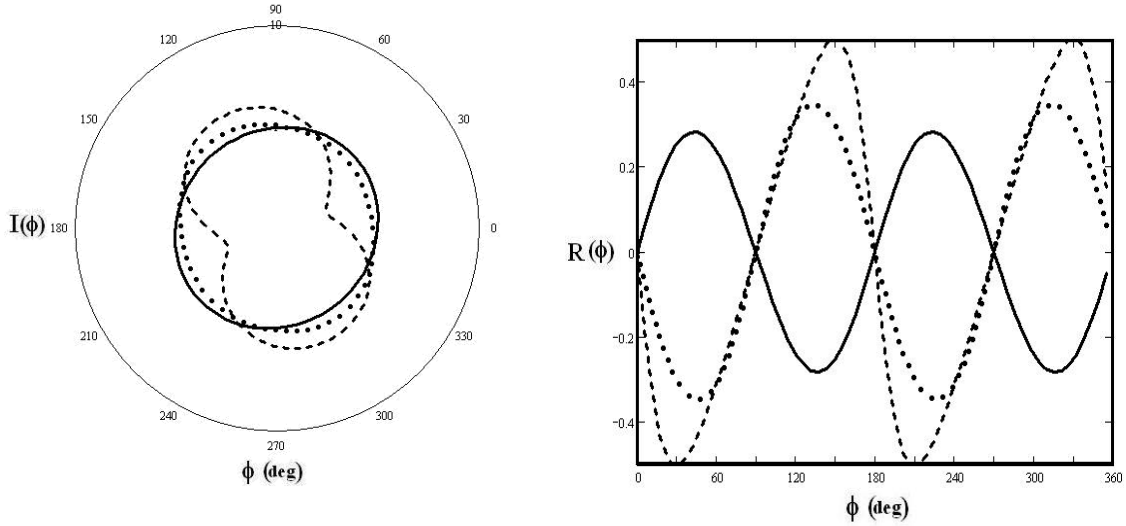

(c)

Fig. 3. The same as in Fig. 1 for the first three curves, but for λ=2420 nm: (a) for H(3s), (b) for H(3p) and (c) for H(3d); the corresponding amplitudes for ζ=40^0 have been multiplied by 10 in (a) and (b), while in (c) for ζ=20^0 and 60^0 the coefficient is 3.

5. CONCLUSION

In the present work, we have shown that the non resonant three photon azimuthal photoelectron angular distribution (PAD) can be analytically expressed in the plane polarization, for initial states with orbital quantum numbers *l*=0,1 and 2 ,

- as: $A_0 + A_2\cos2\phi + A_4\cos4\phi + A_6\cos6\phi + B_2\sin2\phi + B_4\sin4\phi$; where the angular coefficients A_0 A_2, A_4, A_6, B_2 and B_4,depend on the energy and the ellipticity ζ.

This ellipticity depends on two parameters: the elliptic angle χ and the phase difference between the x-semimajor and the y-semiminor axes of the field components.

- It is observed that the expressions of the elliptic dichroism (ED) (the last two terms) built with the phase lag parameter has the same form as that obtained with the elliptic angle. Besides, for *l=0* states and from the phase lag and these ED terms, we have extracted information about the photoelectron energies.
- Furthermore, it has been noted no contribution to the PAD, from the magnetic sublevels *m=0* for *l*=1 ,and *m*=$\pm$1 for *l=2* initial states.

From the numerical results:

- the coefficients, A_0, A_2, A_4, A_6, B_2 and B_4,exhibit the following characteristics :they are all positive or negative, non linear variation; lowest and strongest values for 1s and 3p initial states, respectively; strongest differences between B_2 and B_4 for 3d initial state. For each state, the positive or the negative sign of the B_2, B_4 asymmetric terms, can be explained from the constructive or the destructive interference between the channels associated to the different quantum paths leading to the final states.

- The azimuthal PAD display lobed shapes. The maxima are directed either along the semimajor or along the semiminor axis for 1s, 2s,3s and 3p initial states; they are shifted from these axes, for 2p and 3d states. Except for 3s state, an isotropic shape is also observed for all the others states.

- We have found that, when the maxima for the lobed shapes are directed along these axes, no contribution of the asymmetric terms is noted; but they contribute if the distributions are shifted from them. As to the isotropic shape, it would be due to the relatively high contribution of the isotropic term A_0, with respect to the others coefficients, regardless their sign.

- As for the corresponding ED signals, except for 1s and 2p initial states where four maxima (four minima) have been observed, all exhibit two maxima and two minima. In the case where the photoelectron has a left handed preference, the first maximum is always located at values of the azimuthal angle $\phi \leq 60^0$, while for the case of right handed preference, it is located at $\phi \geq 75^0$.Strongest ED signals observed for 2p, and 3p states, coincide with the minima of the PAD. The highest amplitudes come from the combination of the relatively strong asymmetric terms, associated with a relatively strong destructive second PAD term.

- Furthermore, for 1s state, a nonzero ED signal has been observed for nearly circularly polarized light; a weak ED signal has also been obtained for nearly linearly polarized photons related to the first Born approximation.

These results were obtained for the hydrogen atom, but could give insight into more complex atoms. The extension of these calculations to the total cross section dependence with the both two keys parameters, (the elliptic angle and the phase lag) will be the subject of future work.

ACKNOWLEDGMENTS

This work is dedicated to the memory of Professor. Wane, Sada Tamimou who died recently

REFERENCES

Andrei, Y., Manakov, N.L., Meremianin, A.V., et al. (2004). Circular dichroism at equal energy sharing in photo-double-ionization of Helium. Phys. Rev.A 70, 010702(R)-1-4

Bethe, H.A., Salpeter, E.E. (1957). Methods for the continuous spectrum for a general central potential. Springer Verlag, Quantum Mechanics of One and Two Electron Atoms. Berlin-Göttinen- Heidelberg, pp. 32- 36.

Bouchiat, M.A., Bouchiat, C. (1997). Parity violation in atoms, Rep.Prog.Phys.60, 1351-1396.

Dulieu F., Blondel C., Delsart, C. (1995). Multiphoton angular distributions with elliptically polarized light: II. Three- and four-photon detachment of halogen negative ions. J. Phys. B : At. Mol. Opt. Phys., 28, 3861 - 3871.

Faye, M., Wane, S.T., Ndiaye, S. (2010). Multiphoton angular distribution: occurrence of an isotropic term and effect of light polarization, Int. J. Phys. Sci., 5, 1508-1523.

Faye, M., Wane, S.T., Ndiaye, S. (2003). Non resonant two photon ionization of atomic hydrogen: exact expressions of angular distribution, Phys. Scr., 68, 352- 363

Faye, M., Wane, S.T. (2011a). Phase and ellipticity dependence of the photoelectron angular distribution in non-resonant two photon ionization of atomic hydrogen, J. Phys. B: At. Mol. Opt. Phys., 44, 055204-1-11

Faye, M., Wane, S.T. (2011b). Non resonant two photon ionization of atomic hydrogen with elliptically polarized light: dichroism. Contemporary Problems in Mathematical Physics, ICMPA-UNESCO Chair Publishing, Cotonou, Benin (in press).

Fifirig, M., Florescu, V. (1998). Azimuthal angular distributions for two colour three-photon ionization of hydrogen. Eur. Phys. J. D., 2, 143-147.

Fifirig, M. (2002). Phase and ellipticity dependence of the photoelectrons angular distribution in two-colour ionization. Phys. Scr., 65, 392 - 397.

Godehusen, K. and. Zimmermann, P. (1998). A complete photo ionization experiment with polarized atoms using magnetic dichroism and phase tilt measurements, Phys. Rev. A, 58, R3371-3374.

Huttunen, M.J., et al. (2011). Nonlinear chiral imaging of sub wavelength-sized twisted-cross gold nanodimers, Opt. Mat. Exp., 1, 46-56.

Maquet, A. (1977). Use of the Coulomb Green's function in atomic calculations. Phys. Rev. A, 15, 1088-1108.

Nakajima, T. (2000). Possibility of direct determination of the quantum phase of continua utilizing the phase of lasers, Phys. Rev. A 61, 041403R-1-4

Persoons, A. (2011). Nonlinear optics, chirality, magneto-optics: a serendipitous road. Opt. Mat. Exp., 1, 5-16.

Radhakrishnan, R., Thayyullathil, R.B. (2004). Non resonant multiphoton ionization in atomic hydrogen. Phys. Rev. A, 69, 033407-1-5.

Ricz, S., Ricsoka, T., Kövér, A., et al. (2007). Experimental observation of left-right asymmetry in outer s-shell photo ionization, New J. Phys., 9, 274-1-8.

Viefhaus, J., Avaldi, L., Snell, G., et al. (1996). Experimental Evidence for Circular Dichroism in the Double Photo ionization of Helium. Phys. Rev. Lett., 77, 3975-3978.

APPENDIX

We gather here the explicit expressions of the angular coefficients ($b_{2,ns}$, $b_{4,ns}$) of Eq.(15),($b_{2,np}$, $b_{4,np}$) of Eq.(16), ($b_{2,3d}$}, $b_{4,3d}$) of Eq.(17).

From Eq.(15) one gets:

$$b_{2,ns} = -\frac{1}{48}T_{123}T_{101} - \frac{1}{60}T_{123}T_{121} \quad \text{(A1)}$$

$$b_{4,ns} = -\frac{1}{48}T_{123}T_{101} - \frac{1}{60}T_{123}T_{121} \quad \text{(A2)}$$

From Eq.(16) one obtains:

$$b_{2,np} = \left(\frac{-187}{4200}T_{234}T_{212} - \frac{33}{700}T_{234}T_{232} - \frac{11}{420}T_{234}T_{012}\right)\sin(\delta_4 - \delta_2)$$
$$+\left(\frac{1}{420}T_{234}T_{210} + \frac{1}{336}T_{234}T_{010}\right)\sin(\delta_4 - \delta_0) + \left(-\frac{1}{225}T_{212}T_{210} - \frac{1}{180}T_{212}T_{010}\right.$$

$$\left. -\frac{1}{525}T_{232}T_{210} - \frac{1}{420}T_{232}T_{010} - \frac{1}{36}T_{012}T_{010} - \frac{1}{45}T_{012}T_{210}\right)\sin(\delta_2 - \delta_0) \quad \text{(A3)}$$

and

$$b_{4,np} = \left(\frac{47}{1680}T_{234}T_{212} + \frac{3}{280}T_{234}T_{232} + \frac{1}{168}T_{234}T_{012}\right)\sin(\delta_4 - \delta_2)$$
$$-\left(\frac{1}{60}T_{234}T_{210} + \frac{1}{48}T_{234}T_{010}\right)\sin(\delta_4 - \delta_0) \quad \text{(A4)}$$

From Eq.(17) it comes:

$$b_{2,3d} = \left(-\frac{1831}{8^2 7^2 10}T_{345}T_{323} - \frac{197}{8^2 7^2}T_{345}T_{343} - \frac{701}{8^2 210}T_{345}T_{123}\right)\sin(\delta_5 - \delta_3)$$
$$+\left(\frac{1}{280}T_{345}T_{321} + \frac{37}{1120}T_{345}T_{121} + \frac{5}{504}T_{345}T_{101}\right)\sin(\delta_5 - \delta_1)$$
$$+\left(-\frac{3}{7^2 5^2 8}T_{323}T_{321} - \frac{1}{70}T_{323}T_{121} - \frac{13}{1400}T_{323}T_{101} - \frac{1}{2450}T_{343}T_{321}\right.$$
$$\left. -\frac{17}{5^2 3^2 56}T_{343}T_{121} - \frac{1}{126}T_{343}T_{101} - \frac{1}{600}T_{123}T_{121} - \frac{1}{75}T_{123}T_{101}\right)\sin(\delta_3 - \delta_1) \quad \text{(A5)}$$

and,

$$b_{4,3d} = \left(\frac{53}{7840} T_{345} T_{323} + \frac{9}{1372} T_{345} T_{343} + \frac{37}{3840} T_{345} T_{123} \right) \sin(\delta_5 - \delta_3)$$
$$- \left(\frac{23}{1120} T_{345} T_{321} + \frac{29}{1440} T_{345} T_{121} + \frac{5}{288} T_{345} T_{101} \right) \sin(\delta_5 - \delta_1)$$
$$+ \left(\frac{-3}{7^2 5^2 16} T_{323} T_{321} + \frac{1}{700} T_{323} T_{121} + \frac{1}{80} T_{323} T_{101} + \frac{1}{1960} T_{343} T_{321} \right.$$
$$+ \frac{11}{5040} T_{343} T_{121} + \frac{1}{72} T_{343} T_{101} - \frac{11}{5600} T_{123} T_{321} - \frac{1}{2400} T_{123} T_{121}$$
$$\left. + \frac{1}{96} T_{123} T_{101} \right) \sin(\delta_3 - \delta_1) \qquad \text{(A6)}$$